STANFORD
AERONAUTICS &
ASTRONAUTICS

AA200 Applied Aerodynamics

Chapter 12 - Wings of finite span, lifting line theory constructed using vortex sticks

Brian Cantwell
Department of Aeronautics and Astronautics
Stanford University

Wake vortices

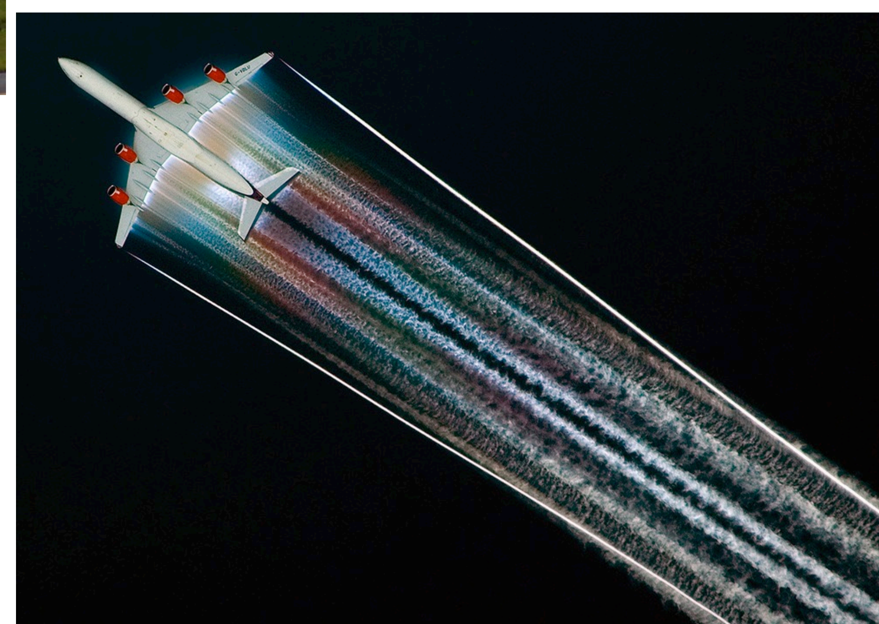

http://i.imgur.com/h8pSK.gif

AA200A Homework 7 2014 -2015
Due Thursday May 28

Read: Chapters 12 and 13

Problem 1 – Take the 2-D wing you studied in Homework 6 and use it as the cross-section of an elliptical planform 3-D wing with aspect ratio 10. Determine the lift, skin friction drag, induced drag and moment coefficients of the wing for several angles of attack. Ignore possible cross-flow effects.

Problem 2 – Estimate the effect on the pressure distribution and lift if the wing in problem 1 is flown at a Mach number of 0.5.

12.1 Flow over a three-dimensional wing

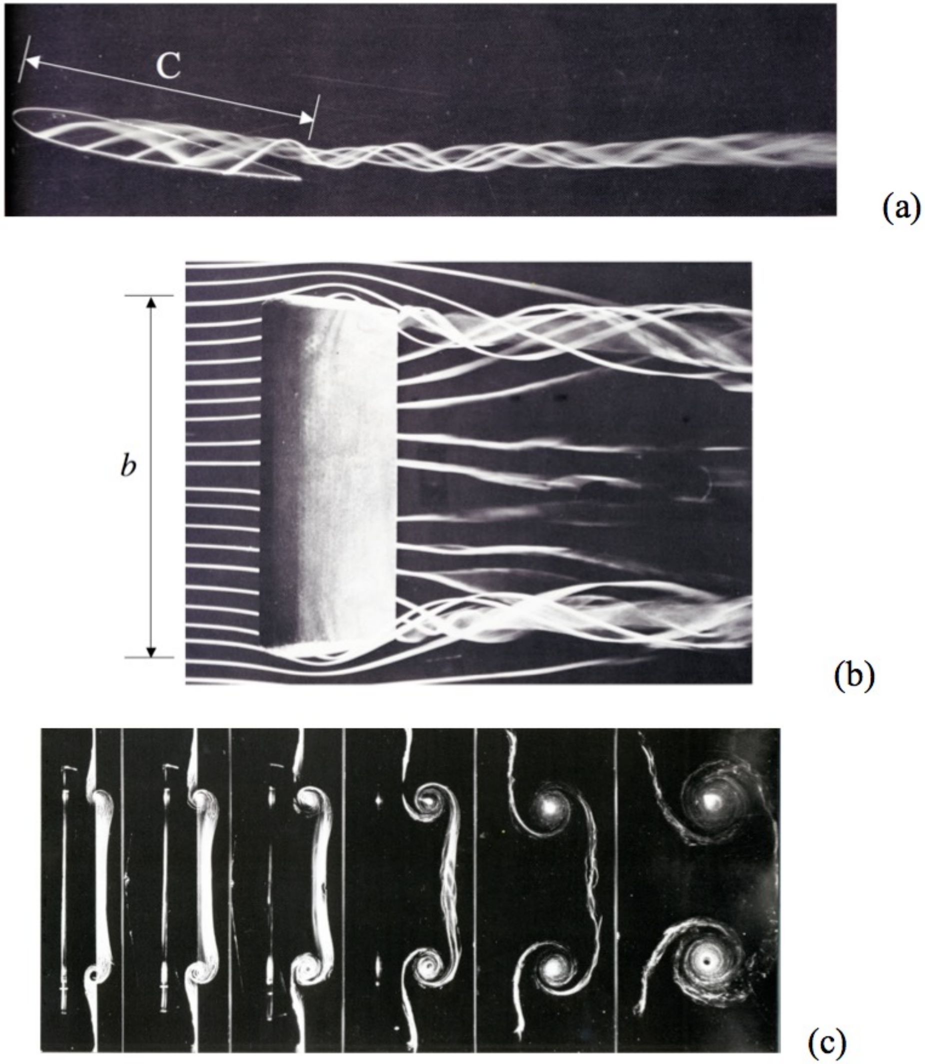

Figure 12.1 Images of the flow past a finite span wing at low speed. From An Album of Fluid Motion by M. Van Dyke.

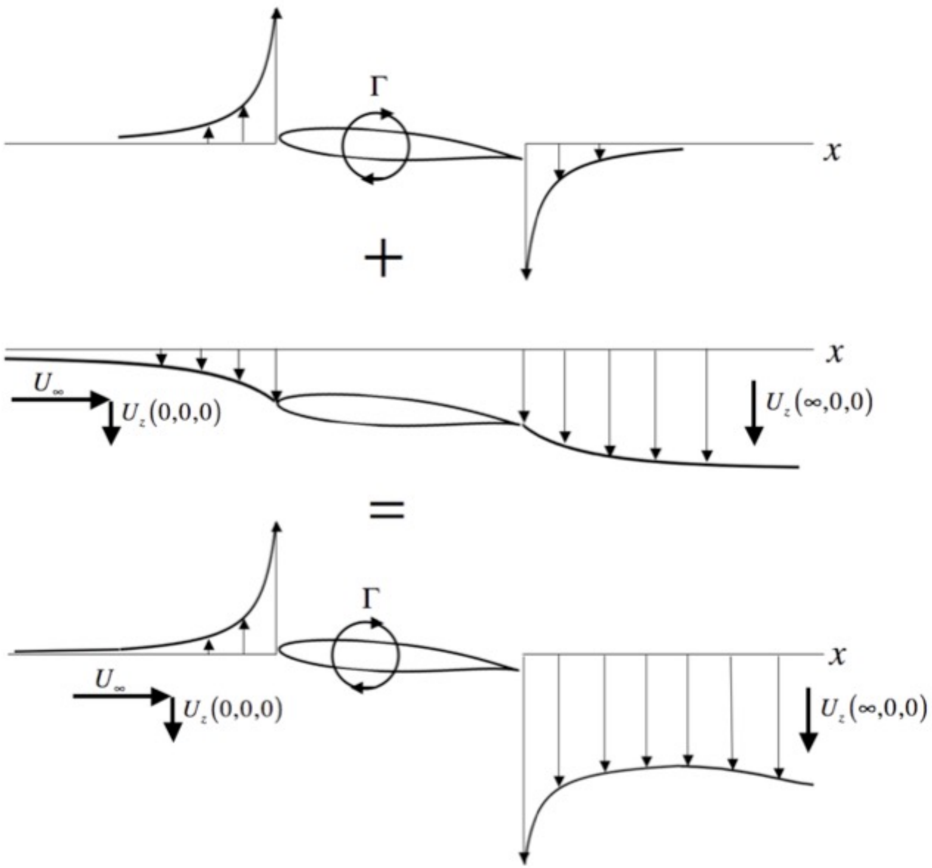

Figure 12.2 – Velocity field normal to a wing comprising a transverse bound vortex of circulation Γ plus downwash generated by a semi-infinite system of free vortices in the wake.

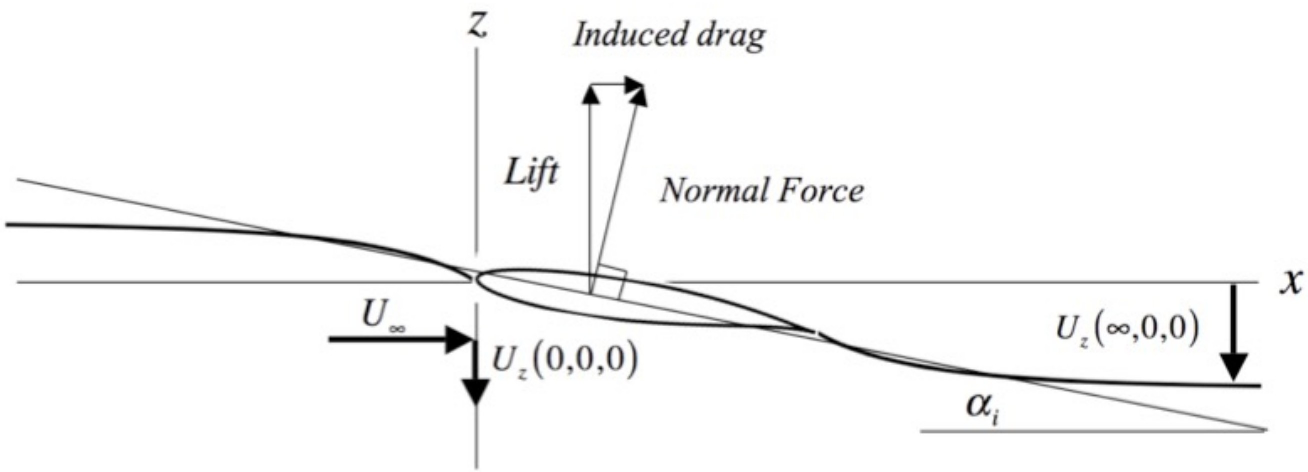

Figure 12.3 Upstream and downstream effect of the wake of a finite span lifting wing.

$$\alpha_i = ArcTan\left(\frac{U_z(0,0,0)}{U_\infty}\right) < 0 \qquad (12.1)$$

Spanwise flow above the wing is toward the centerline

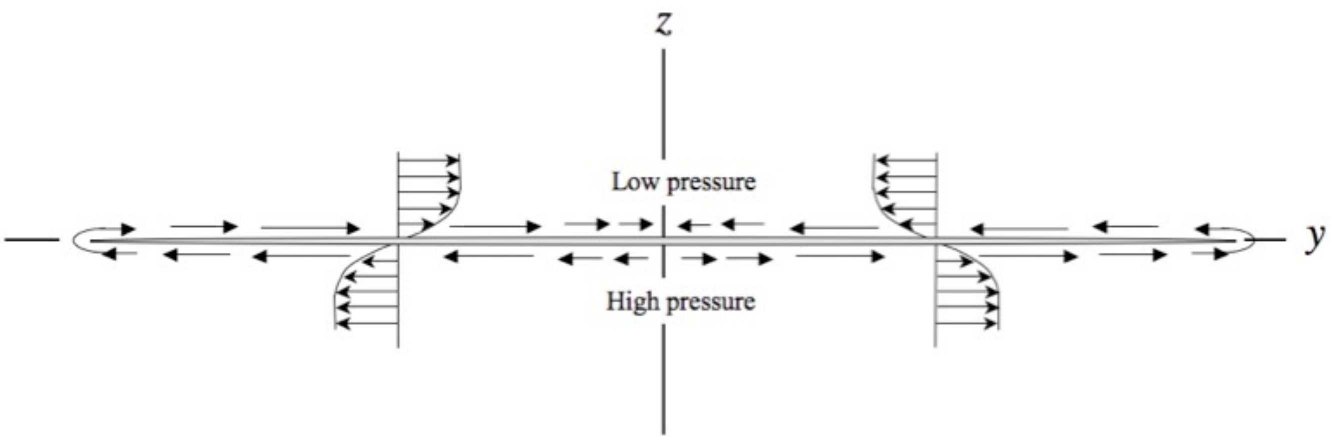

Figure 12.4 Span-wise flow in a plane perpendicular to the wing trailing edge

Spanwise flow below the wing is away from the centerline

Circulation on the wing and circulation at the trailing edge are connected

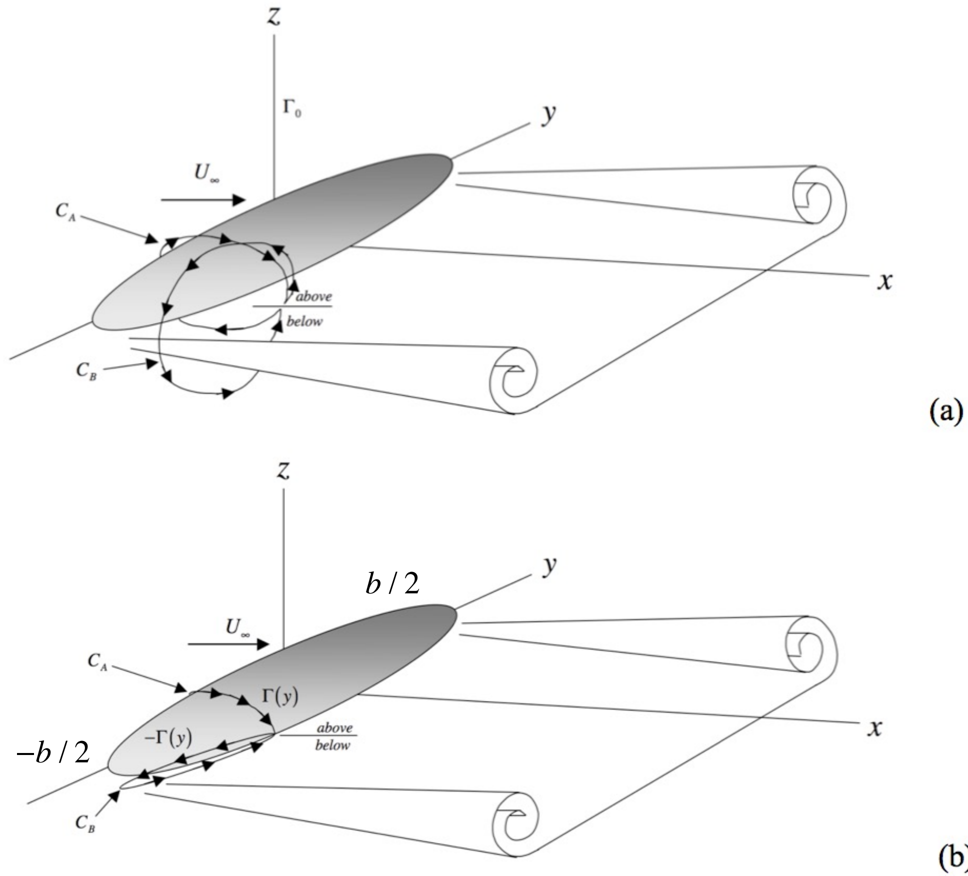

Figure 12.5 Contour used to connect the circulation bound to a lifting wing, the span-wise flow at the wing trailing edge and free vorticity in the wake.

$$\oint \bar{U} \bullet \hat{c}\, dC = \oint \nabla\Phi \bullet \hat{c}\, dC = \oint d\Phi = \Phi_{final} - \Phi_{initial} = 0 \qquad (12.2)$$

$$\oint \bar{U} \bullet \hat{c}\, dC = \int_{C_A} \bar{U} \bullet \hat{c}\, dC + \int_{C_B} \bar{U} \bullet \hat{c}\, dC = 0 \qquad (12.3)$$

$$\Gamma_{TrailingEdge}(y) = -\Gamma_{Wing}(y) \qquad (12.4)$$

12.2 Circulation and pressure

Linearized derivation of the relation between circulation and pressure.

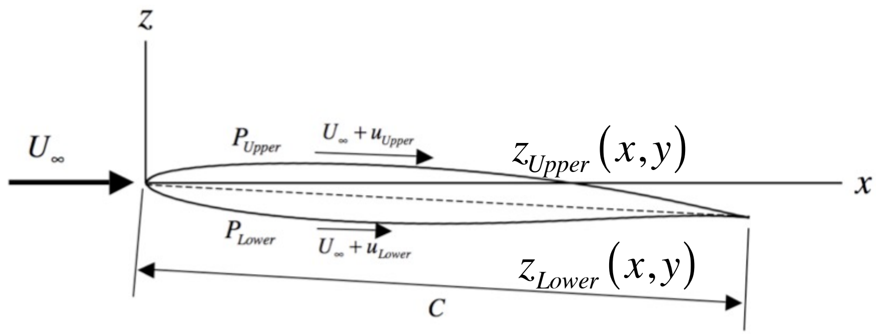

Figure 12.6 Airfoil cross-section

$$\frac{dL}{dy} = \int_0^{C(y)} \left(P_{Lower} \left(\frac{1}{\left(1 + \left(\frac{dz_{Lower}}{dx}\right)^2\right)^{1/2}} \right) - P_{Upper} \left(\frac{1}{\left(1 + \left(\frac{dz_{Upper}}{dx}\right)^2\right)^{1/2}} \right) \right) dx \qquad (12.5)$$

$$P_\infty + \frac{1}{2}\rho U_\infty^2 = P_{Lower} + \frac{1}{2}\rho \left(U_{Lower}\right)^2 = P_{Upper} + \frac{1}{2}\rho\left(U_{Upper}\right)^2 \qquad (12.6)$$

$$P_\infty + \cancel{\frac{1}{2}\rho U_\infty^2} \cong P_{Lower} + \rho U_\infty u_{Lower} = P_{Upper} + \rho U_\infty u_{Upper} \qquad (12.7)$$

$$\frac{dL}{dy} = \rho U_\infty \int_0^C \left(u_{Upper} - u_{Lower}\right) dx = \rho U_\infty \Gamma(y) \qquad (12.8)$$

$$\Gamma = \oint_C \bar{U} \bullet \hat{c}\, dC \qquad (12.9)$$

12.3 Forces and moments on a 3-D wing

Recall eqn 10.145

$$\bar{F}_{\perp} = -\rho \bar{U}_R \times \int_{A_w} \nabla\Phi \times \hat{n}\, dA$$

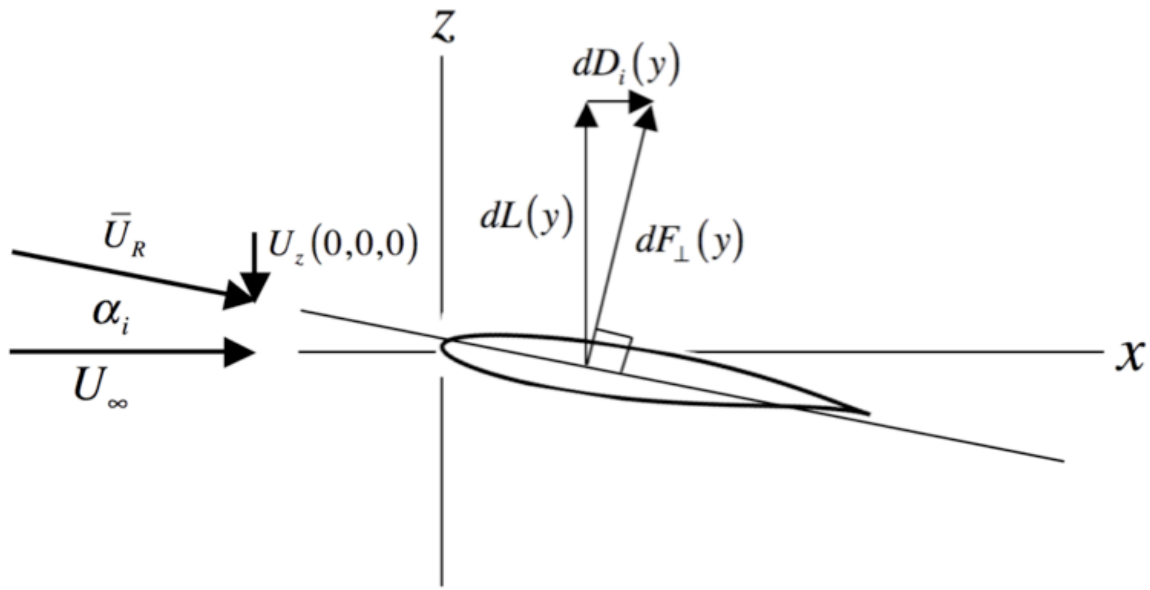

Fig 12.7 Differential forces on a section of a 3-D wing

$$dF_{\perp}(y) = \rho U_R(y)\Gamma(y)dy \tag{12.10}$$

$$dL(y) = dF_{\perp}(y)Cos(\alpha_i) = dF_{\perp}(y)\frac{U_{\infty}}{U_R(0,y,0)} = \rho U_{\infty}\Gamma(y)dy \tag{12.11}$$

$$dD_i(y) = -dF_{\perp}(y)Sin(\alpha_i) = -dF_{\perp}(y)\frac{U_z(0,y,0)}{U_R(0,y,0)} = -\rho U_z(0,y,0)\Gamma(y)dy \tag{12.12}$$

$$dD_i(y) = -\alpha_i(y)\,dL(y) \tag{12.13}$$

$$L = \rho U_\infty \int_{-b/2}^{b/2} \Gamma(y)\,dy \tag{12.14}$$

$$D_i = -\rho \int_{-b/2}^{b/2} U_z(0,y,0)\,\Gamma(y)\,dy \tag{12.15}$$

$$M_x = M_{Roll} = \int_{-b/2}^{b/2} y\,dL(y) = \rho U_\infty \int_{-b/2}^{b/2} y\Gamma(y)\,dy \tag{12.16}$$

$$M_z = M_{Yaw} = -\int_{-b/2}^{b/2} y\,dD_i(y) = \rho \int_{-b/2}^{b/2} yU_z(0,y,0)\Gamma(y)\,dy \tag{12.17}$$

$$M_y = \rho U_\infty \int_{-b/2}^{b/2} \int_0^C x\gamma(x,y)\,dx\,dy$$

Total pitching moment is determined by integrating the 2-D section pitching moment along the span.

12.4 Lifting line theory, vortex sticks

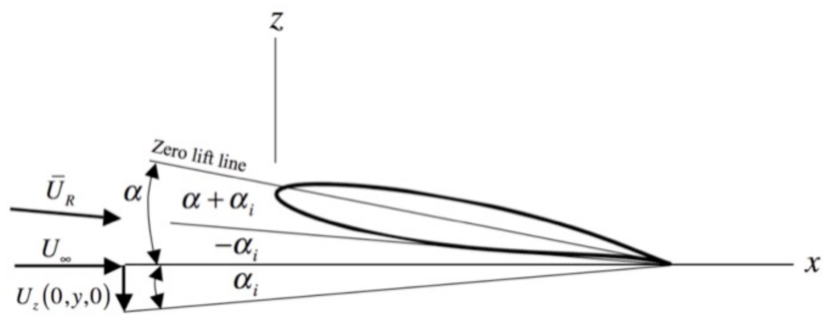

Figure 12.8 Wing cross section at spanwise position y.

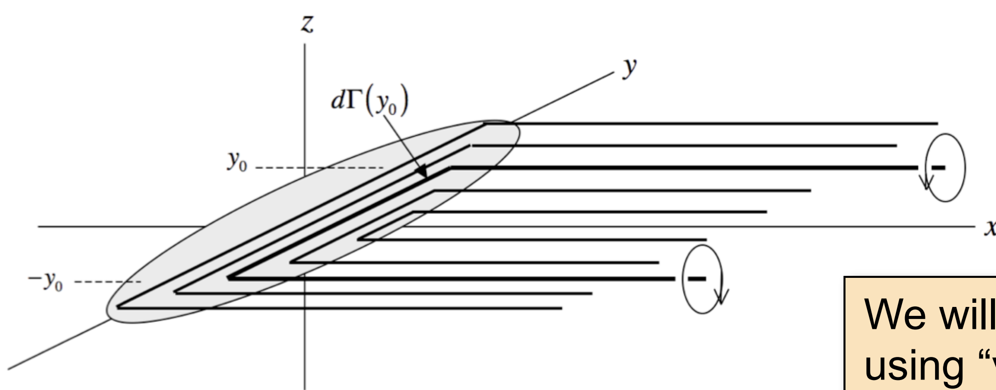

We will construct the wake using "vortex sticks".

Figure 12.9 Wing and trailing vortex sheet model for inviscid lifting line theory.

Wing aspect ratio

$$A_R = \frac{b^2}{S} \tag{12.18}$$

Relative velocity vector

$$\bar{U}_R(0,y,0) = \{U_\infty, 0, U_z(0,y,0)\} \tag{12.19}$$

Recall the Poisson equation for the vector potential

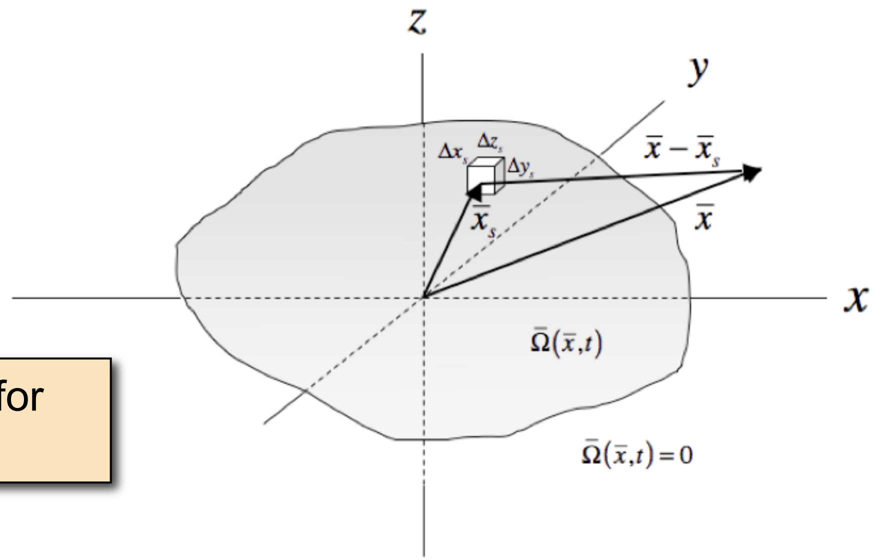

Figure 12.10 Vorticity source distribution surrounded by irrotational flow

$$\nabla^2 \bar{A}(x,y,z,t) = -\bar{\Omega}(x,y,z,t) \qquad (12.20)$$

$$\nabla^2 A_x = -\Omega_x \qquad \nabla^2 A_y = -\Omega_y \qquad \nabla^2 A_z = -\Omega_z \qquad (12.21)$$

$$d\bar{A} = -\frac{\bar{\Omega}(\bar{x}_s,t)\,dx_s dy_s dz_s}{4\pi\left|\bar{x}-\bar{x}_s\right|} \qquad (12.22)$$

$$\bar{A}(\bar{x},t) = \frac{1}{4\pi}\int_{-\infty}^{\infty}\int_{-\infty}^{\infty}\int_{-\infty}^{\infty}\frac{\bar{\Omega}(\bar{x}_s,t)}{\left|\bar{x}-\bar{x}_s\right|}dx_s\,dy_s\,dz_s \qquad (12.23)$$

Vector potential of two semi-infinite lines of vortex monopoles;
semi-infinite vortex sticks

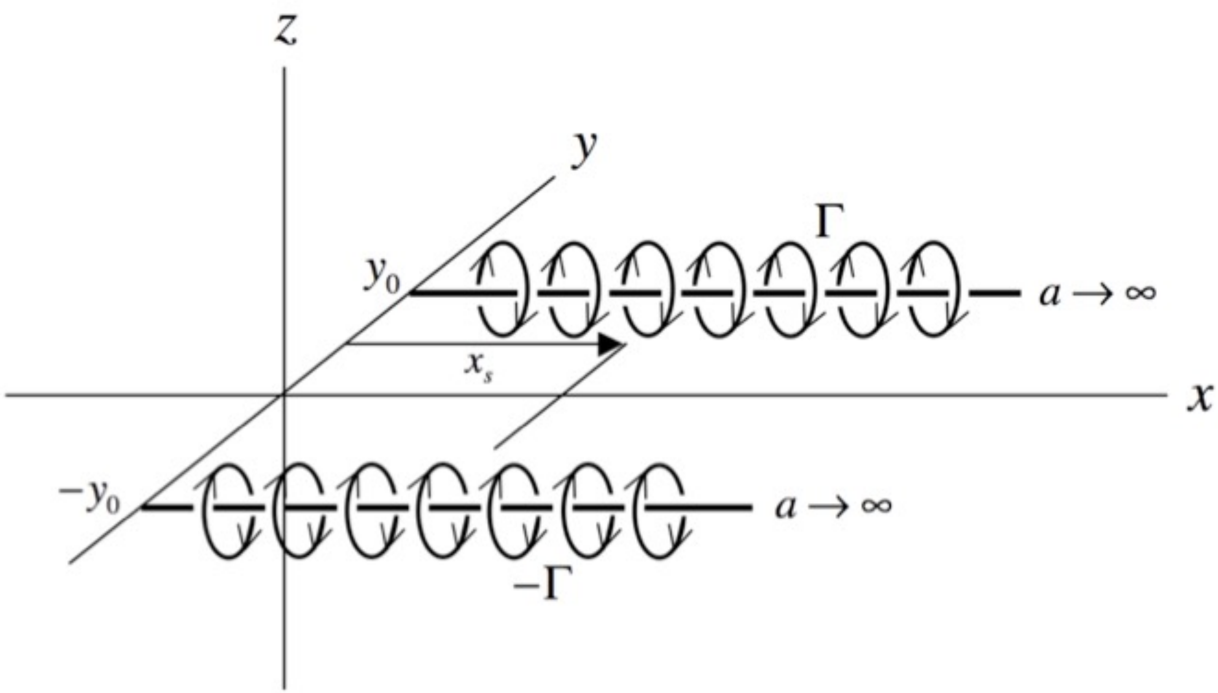

Figure 12.11 Two parallel semi-infinite vortex lines of opposite sign

STANFORD AERONAUTICS & ASTRONAUTICS

Semi-infinite vortex line at $+y_0$

$$\bar{\Omega}^{+}(\bar{x},t)=\left\{\Gamma u(x)\delta(y-y_0)\delta(z),0,0\right\} \tag{12.24}$$

$$A_x^{+}=\frac{1}{4\pi}\int_{-\infty}^{\infty}\int_{-\infty}^{\infty}\int_{-\infty}^{\infty}\frac{\Gamma u(x_s)\delta(y_s-y_0)\delta(z_s)}{\left((x-x_s)^2+(y-y_s)^2+(z-z_s)^2\right)^{1/2}}dx_s\,dy_s\,dz_s=$$

$$\frac{1}{4\pi}\int_{0}^{\infty}\frac{\Gamma}{\left((x-x_s)^2+(y-y_0)^2+z^2\right)^{1/2}}dx_s=\lim_{a\to\infty}\frac{-\Gamma}{4\pi}Ln\left(\frac{x-a+\sqrt{(x-a)^2+(y-y_0)^2+z^2}}{x+\sqrt{x^2+(y-y_0)^2+z^2}}\right) \tag{12.25}$$

$$A_x^{+}=\frac{\Gamma}{4\pi}\left(Ln\left(x+\sqrt{x^2+(y-y_0)^2+z^2}\right)-Ln\left((y-y_0)^2+z^2\right)-\lim_{a\to\infty}Ln\left(\frac{1}{2a}\right)\right) \tag{12.26}$$

Semi-infinite vortex line at $-y_0$

$$\bar{\Omega}^{-}(\bar{x}) = \left\{-\Gamma u(x)\delta(y+y_0)\delta(z), 0, 0\right\} \tag{12.27}$$

$$A_x^{-} = \frac{1}{4\pi}\int_{-\infty}^{\infty}\int_{-\infty}^{\infty}\int_{-\infty}^{\infty}\frac{-\Gamma u(x_s)\delta(y_s+y_0)\delta(z_s)}{\left((x-x_s)^2+(y-y_s)^2+(z-z_s)^2\right)^{1/2}}dx_s\,dy_s\,dz_s =$$

$$\frac{-1}{4\pi}\int_0^{\infty}\frac{\Gamma}{\left((x-x_s)^2+(y+y_0)^2+z^2\right)^{1/2}}dz_s = \lim_{a\to\infty}\frac{\Gamma}{4\pi}Ln\left(\frac{x-a+\sqrt{(x-a)^2+(y+y_0)^2+z^2}}{x+\sqrt{x^2+(y+y_0)^2+z^2}}\right)$$

$$(12.28)$$

$$A_x^{-} = \frac{\Gamma}{4\pi}\left(-Ln\left(x+\sqrt{x^2+(y+y_0)^2+z^2}\right)+Ln\left((y+y_0)^2+z^2\right)+\lim_{a\to\infty}Ln\left(\frac{1}{2a}\right)\right) \tag{12.29}$$

Superpose the vector potentials of the two vortex lines

$$A_x = \frac{-\Gamma}{4\pi} Ln\left(\frac{x + \left(x^2 + \left(y + y_0\right)^2 + z^2\right)^{1/2}\left(\left(y - y_0\right)^2 + z^2\right)}{\left(x + \left(x^2 + \left(y - y_0\right)^2 + z^2\right)^{1/2}\right)\left(\left(y + y_0\right)^2 + z^2\right)} \right) \tag{12.30}$$

Velocity field

$$U_y = \frac{-\Gamma}{4\pi}\left(\begin{array}{l} \dfrac{-z\left(\left(y+y_0\right)^2+z^2\right) - 2z\left(x+\left(x^2+\left(y-y_0\right)^2+z^2\right)^{1/2}\right)\left(x^2+\left(y-y_0\right)^2+z^2\right)^{1/2}}{\left(x^2+\left(y-y_0\right)^2+z^2\right)^{1/2}\left(x+\left(x^2+\left(y-y_0\right)^2+z^2\right)^{1/2}\right)\left(\left(y+y_0\right)^2+z^2\right)} + \\ \dfrac{z\left(\left(y-y_0\right)^2+z^2\right) + 2z\left(x+\left(x^2+\left(y+y_0\right)^2+z^2\right)^{1/2}\right)\left(x^2+\left(y+y_0\right)^2+z^2\right)^{1/2}}{\left(x^2+\left(y+y_0\right)^2+z^2\right)^{1/2}\left(x+\left(x^2+\left(y+y_0\right)^2+z^2\right)^{1/2}\right)\left(\left(y-y_0\right)^2+z^2\right)} \end{array} \right)$$

$$U_z = \frac{\Gamma}{4\pi}\left(\begin{array}{l} \dfrac{-\left(y-y_0\right)\left(\left(y+y_0\right)^2+z^2\right) - 2\left(y+y_0\right)\left(x+\left(x^2+\left(y-y_0\right)^2+z^2\right)^{1/2}\right)\left(x^2+\left(y-y_0\right)^2+z^2\right)^{1/2}}{\left(x^2+\left(y-y_0\right)^2+z^2\right)^{1/2}\left(x+\left(x^2+\left(y-y_0\right)^2+z^2\right)^{1/2}\right)\left(\left(y+y_0\right)^2+z^2\right)} + \\ \dfrac{\left(y+y_0\right)\left(\left(y-y_0\right)^2+z^2\right) + 2\left(y-y_0\right)\left(x+\left(x^2+\left(y+y_0\right)^2+z^2\right)^{1/2}\right)\left(x^2+\left(y+y_0\right)^2+z^2\right)^{1/2}}{\left(x^2+\left(y+y_0\right)^2+z^2\right)^{1/2}\left(x+\left(x^2+\left(y+y_0\right)^2+z^2\right)^{1/2}\right)\left(\left(y-y_0\right)^2+z^2\right)} \end{array} \right)$$

(12.31)

Downwash velocity at the lifting line due to two semi-infinite vortex lines

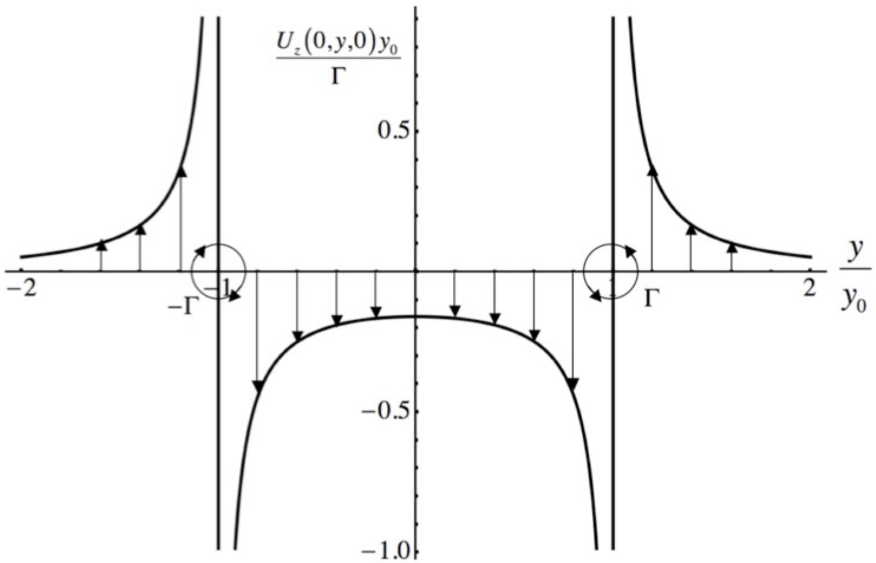

Figure 12.12 Downwash induced by two parallel semi-infinite vortex lines of opposite sign on the line $\{x,z\}=\{0,0\}$ *viewed from the vortex wake (positive x).*

$$U_z(0,y,0)=\frac{\Gamma}{2\pi}\left(\frac{y_0}{\left(y^2-y_0^2\right)}\right) \tag{12.32}$$

$$U_z(0,0,0)=-\frac{\Gamma}{2\pi y_0} \tag{12.33}$$

$$U_z(x,0,0) = \frac{\Gamma}{2\pi y_0}\left(\frac{1-2\left(x/y_0+\left(1+(x/y_0)^2\right)^{1/2}\right)\left(1+(x/y_0)^2\right)^{1/2}}{\left(1+(x/y_0)^2\right)^{1/2}\left(x/y_0+\left(1+(x/y_0)^2\right)^{1/2}\right)}\right) \tag{12.34}$$

$$\lim_{x\to\infty} U_z(x,0,0) = -\frac{\Gamma}{\pi y_0} \qquad \cancel{\lim_{z\to-\infty} U_y(0,0,z) = -\frac{\Gamma}{\pi y_0}} \tag{12.35}$$

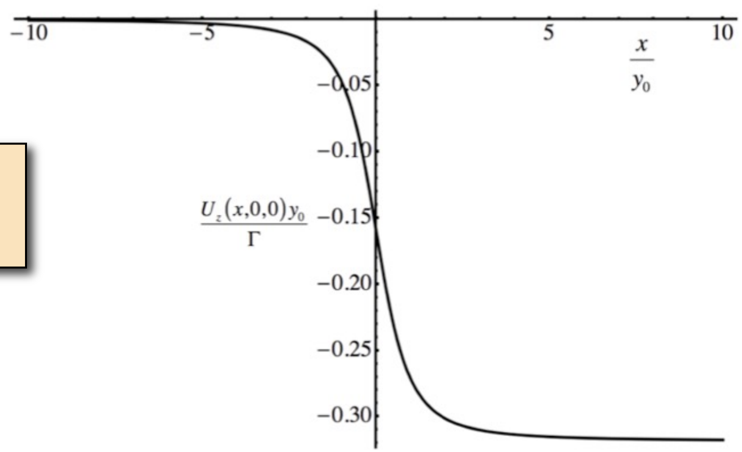

Downwash velocity along the centerline of the flow

Figure 12.13 Downwash induced by two parallel semi-infinite vortex lines of opposite sign on the line $\{y,z\}=\{0,0\}$.

The idea of building flows using “vortex sticks” has been used to try to model hairpin vortices observed in turbulent boundary layers.

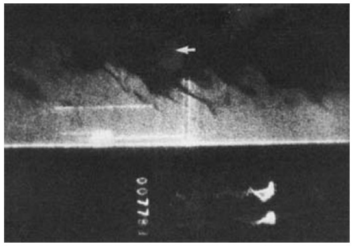

FIGURE 4. Simultaneous passage of interface past two hot wire

FIGURE 38. Example of curled-over hairpin in developing spot.

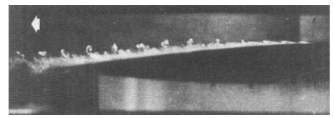

FIGURE 39. Succession of curled-over hairpins photographed by Bergh (1957).

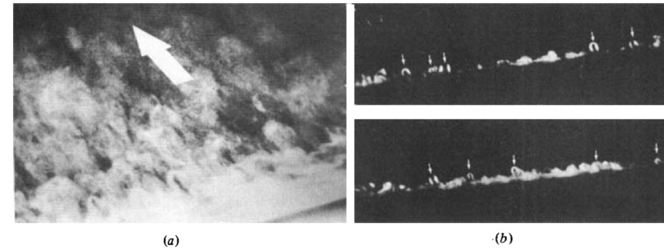

FIGURE 6. Horseshoe vortices in reattaching flow behind circular rod. (a) General illumination, (b) illumination by transverse light plane.

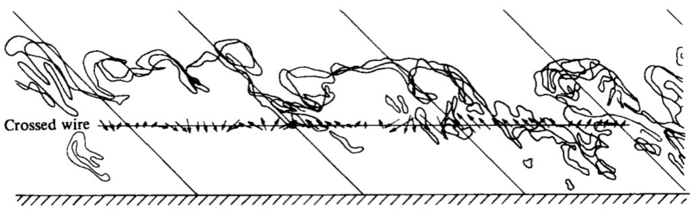

FIGURE 5. Vector plot of disturbance velocities with the edge of the smoke indicated.

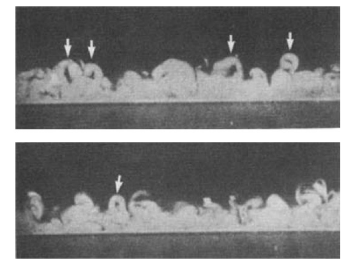

FIGURE 7. Horseshoe vortices in low-Reynolds-number boundary layer (cross-stream illumination, $Re_\theta \simeq 500$).

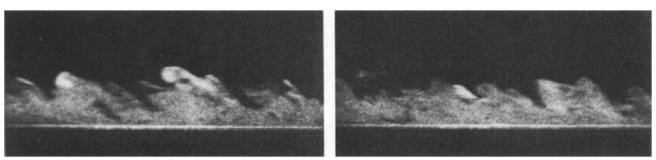

FIGURE 16. Boundary-layer structure at a low Reynolds number ($Re_\theta \simeq 500$; see also figure 34).

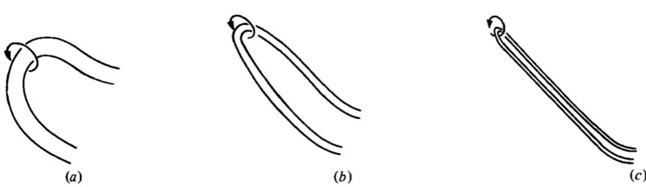

FIGURE 17. Effect of Reynolds number on features composing an outer region of turbulent boundary layer. (a) *Very* low *Re* (loops); (b) low–moderate *Re* (elongated loops or horseshoes); (c) moderate–high *Re* (elongated hairpins or vortex pairs).

82 *Wallace et al.*

FIGURE 6. (a) Hairpin vortex in developed turbulence at $Re_\theta = 1850$ indicated by isosurfaces of Q. (b) Closeup of highlighted hairpin with vorticity lines superimposed.

New aspects of turbulent boundary-layer structure - M. R. Head and P. Bandyopadhyay – JFM Vol 107 1981

Boundary layer turbulence in transitional and developed states – Wallace, Park, Wu and Moin – CTR Summer Program 2010

Vortex stick model of turbulent boundary layers.

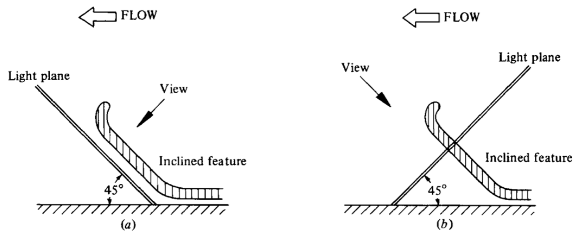

FIGURE 18. Inclined features being convected past light plane. (a) Downstream light plane; (b) upstream light plane.

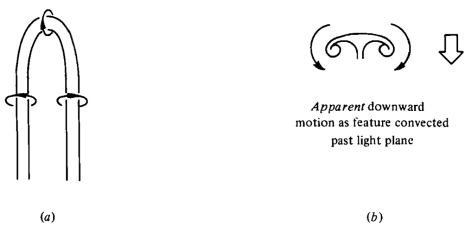

FIGURE 19. Views seen by camera as feature convected past light plane. (a) 45° downstream light plane; (b) 45° upstream light plane.

New aspects of turbulent boundary-layer structure - M. R. Head and P. Bandyopadhyay – JFM Vol 107 1981

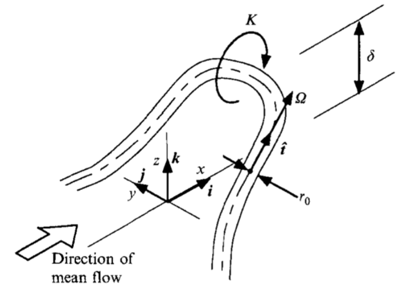

FIGURE 2. Sketch of a representative attached eddy.

A wall-wake model for the turbulence structure of boundary layers. Part 1. Extension of the attached eddy hypothesis – Perry and Marusic – JFM Vol 298 1995

Theoretical and experimental study of wall turbulence 167

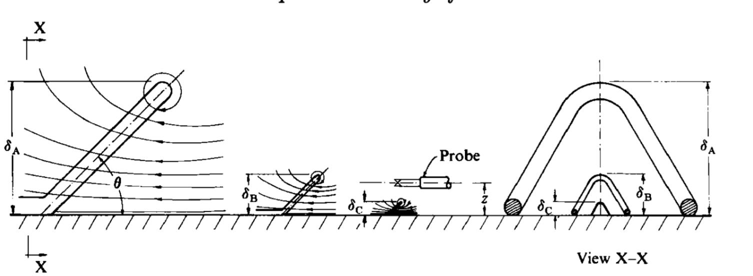

FIGURE 1. A sketch of three attached eddies of varying scales together with the instantaneous streamline pattern generated by each.

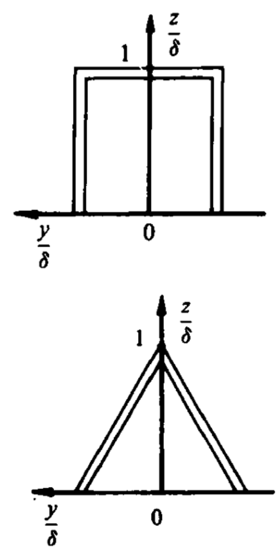

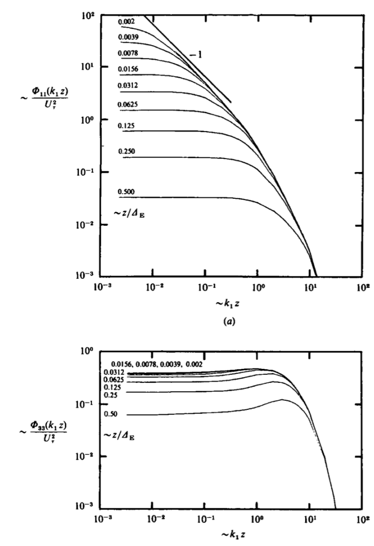

FIGURE 25. Spectra computed using the Λ-vortex model for varying values of z/Δ_E scaled with 'inner-flow'-scaling coordinates. (a) u_1 spectra. (b) u_2 spectra.

A theoretical and experimental study of wall turbulence - Perry, Henbest and Chong – JFM Vol 165 1986

Downwash due to a sheet of vorticity shed into the wake of the airfoil

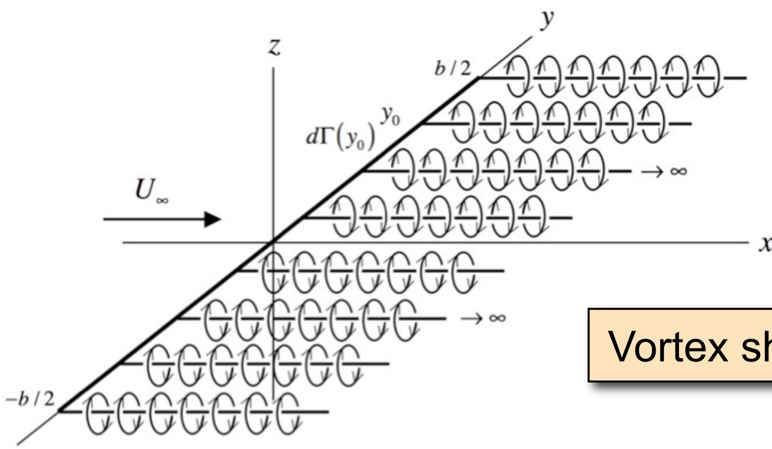

Figure 12.14 Continuous distribution of vortex lines attached to the y-axis.

Vortex sheet lies in the (x,y) plane

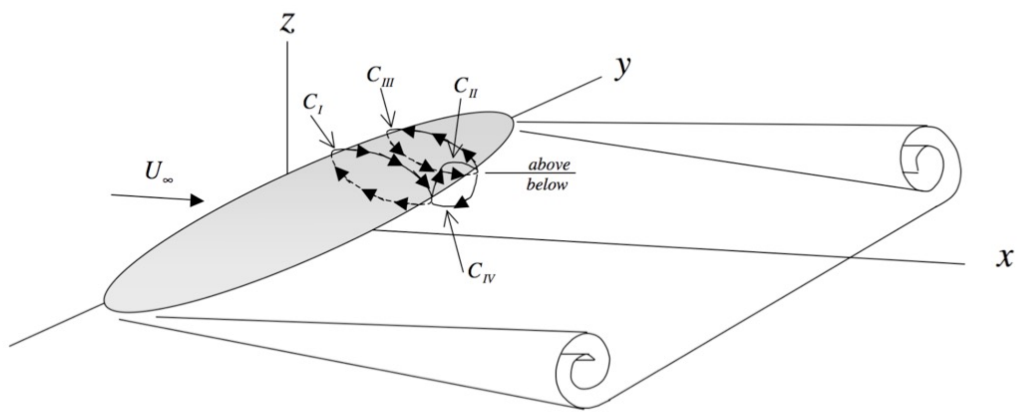

Figure 12.15 Contour used to relate the incremental circulation on the wing to the incremental circulation shed into the wake

Differential strength of the vortex sheet

$$\oint \bar{U} \bullet \hat{c}\, dC = \int_{C_I} \bar{U} \bullet \hat{c}\, dC + \int_{C_{II}} \bar{U} \bullet \hat{c}\, dC + \int_{C_{III}} \bar{U} \bullet \hat{c}\, dC + \int_{C_{IV}} \bar{U} \bullet \hat{c}\, dC = 0 \tag{12.36}$$

$$\int_{C_I} \bar{U} \bullet \hat{c}\, dC = \Gamma > 0$$

$$\int_{CIII} \bar{U} \bullet \hat{c}\, dC = -\Gamma - \frac{d\Gamma}{dy} dy \tag{12.37}$$

$$\int_{C_{II}} \bar{U} \bullet \hat{c}\, dC + \int_{C_{IV}} \bar{U} \bullet \hat{c}\, dC = -\frac{d\Gamma_{T.E}}{dy} dy$$

$$d\Gamma_{T.E.} = -d\Gamma \tag{12.38}$$

Vector potential of the vortex sheet

$$dA_x = \frac{1}{4\pi} d\Gamma_{T.E.}(y_0) Ln\left(\frac{\left(x+\left(x^2+(y-y_0)^2+z^2\right)^{1/2}\right)}{\left((y-y_0)^2+z^2\right)}\right) \tag{12.39}$$

$$dA_x = -\frac{1}{4\pi} d\Gamma(y_0) Ln\left(\frac{\left(x+\left(x^2+(y-y_0)^2+z^2\right)^{1/2}\right)}{\left((y-y_0)^2+z^2\right)}\right) \tag{12.40}$$

$$A_x = -\frac{1}{4\pi}\int_{-b/2}^{b/2} \frac{d\Gamma(y_0)}{dy_0} Ln\left(\frac{\left(x+\left(x^2+(y-y_0)^2+z^2\right)^{1/2}\right)}{\left((y-y_0)^2+z^2\right)}\right) dy_0 \tag{12.41}$$

STANFORD AERONAUTICS & ASTRONAUTICS

Velocity field of the vortex sheet

$$U_y(x,y,z) = -\frac{1}{4\pi}\int_{-b/2}^{b/2}\frac{d\Gamma}{dy_0}\times$$

$$\left(\frac{z\left((y-y_0)^2+z^2\right)^2 - 2z\left(x+\left(x^2+(y-y_0)^2+z^2\right)^{1/2}\right)\left(x^2+(y-y_0)^2+z^2\right)^{1/2}\left((y-y_0)^2+z^2\right)}{\left(x^2+(y-y_0)^2+z^2\right)^{1/2}\left(x+\left(x^2+(y-y_0)^2+z^2\right)^{1/2}\right)\left((y-y_0)^2+z^2\right)^2}\right)dy_0$$

$$U_z(x,y,z) = \frac{1}{4\pi}\int_{-b/2}^{b/2}\frac{d\Gamma}{dy_0}\times$$

$$\left(\frac{(y-y_0)\left((y-y_0)^2+z^2\right)^2 - 2(y-y_0)\left(x+\left(x^2+(y-y_0)^2+z^2\right)^{1/2}\right)\left(x^2+(y-y_0)^2+z^2\right)^{1/2}\left((y-y_0)^2+z^2\right)}{\left(x^2+(y-y_0)^2+z^2\right)^{1/2}\left(x+\left(x^2+(y-y_0)^2+z^2\right)^{1/2}\right)\left((y-y_0)^2+z^2\right)^2}\right)dy_0$$

(12.42)

Recall the induced drag in 2-D due to a starting vortex

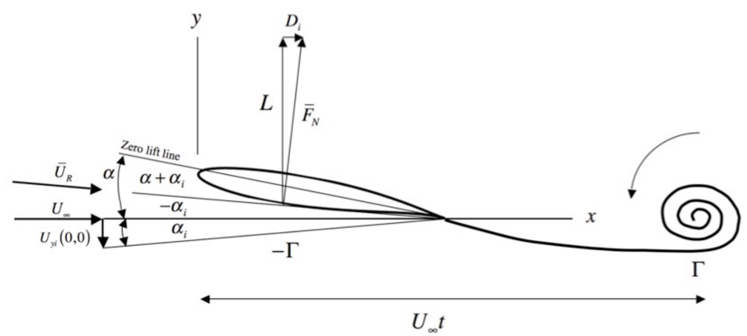

Fig 11.3 Effect of starting vortex downwash on lift and drag of an airfoil.

We worked out an equation for the circulation based on the modified angle of attack induced by the starting vortex.

$$C_L = \frac{L}{\frac{1}{2}\rho U_\infty^2 C} = a_0\left(\alpha + \alpha_i\right) \qquad (11.16)$$

$$-\rho U_\infty \Gamma_{Wing} = a_0 \frac{1}{2}\rho U_\infty^2 C\left(\alpha + \frac{\Gamma_{Wing}}{2\pi U_\infty^2 t}\right). \qquad (11.17)$$

$$\frac{-2\Gamma_{Wing}(t)}{U_\infty C} = \left(\frac{\dfrac{4\pi U_\infty t}{a_0 C}}{\dfrac{4\pi U_\infty t}{a_0 C}+1}\right)a_0\alpha = C_L(t) \qquad (11.18)$$

12.5 Prandtl's equation of finite wing theory

The velocity vector on the lifting line is

$$\bar{U}_R = \left(U_\infty, 0, U_z\right)$$

Downwash velocity along the lifting line

$$U_z(0,y,0) = -\frac{1}{4\pi}\int_{-b/2}^{b/2}\left(\frac{d\Gamma(y_0)}{dy_0}\right)\left(\frac{1}{y-y_0}\right)dy_0 \qquad (12.43)$$

Relative flow velocity approaching the wing

$$U_R(y) = \left(U_\infty^2 + U_z(0,y,0)^2\right)^{1/2} \qquad (12.44)$$

Relative angle of attack of the velocity vector approaching the wing

$$\alpha_R(y) = \alpha(y) + \alpha_i(y) \qquad (12.45)$$

Reduction in angle of attack due to the induced velocity at the lifting line

$$\alpha_i(y) = ArcTan\left(\frac{U_z(0,y,0)}{U_\infty}\right) < 0 \qquad (12.46)$$

At small angle of attack the circulation about an infinite wing is

$$C_L = a_0\alpha_R$$

$$\frac{L}{\frac{1}{2}\rho U_R^2 C} = a_0\alpha_R$$

$$\rho U_R \Gamma = \frac{1}{2}\rho U_R^2 C a_0 \alpha_R$$

$$\Gamma = \frac{1}{2}a_0 C U_R \alpha_R$$

$$\Gamma(y) = K(y)U_R(y)\alpha_R(y) \qquad (12.47)$$

Wing shape factor depends on airfoil form – 2-D theory tells us

$$K(y) = \frac{1}{2}a_0(y)C(y) \qquad (12.48)$$

Lift curve slope of an infinite (2D) wing of the given cross section at the spanwise position y

$$a_0(y) = \left(\frac{dC_L}{d\alpha}(y)\right) \qquad (12.49)$$

STANFORD AERONAUTICS & ASTRONAUTICS

Combine relations

$$\Gamma(y)=\frac{1}{2}a_0(y)C(y)U_R(y)\times$$
$$\left(\alpha(y)-ArcTan\left(\frac{1}{4\pi U_\infty}\int_{-b/2}^{b/2}\left(\frac{d\Gamma(y_0)}{dy_0}\right)\left(\frac{1}{(y-y_0)}\right)dy_0\right)\right) \qquad (12.50)$$

Simplify $U_R \cong U_\infty \qquad \alpha_i \cong U_z / U_\infty$

Prandtl's equation of finite wing theory - an integro-differential equation for the circulation.

$$\Gamma(y)=\frac{1}{2}a_0(y)C(y)\left(U_\infty\alpha(y)-\frac{1}{4\pi}\int_{-b/2}^{b/2}\left(\frac{d\Gamma(y_0)}{dy_0}\right)\left(\frac{1}{(y-y_0)}\right)dy_0\right) \qquad (12.51)$$

Solve subject to the condition that the circulation goes to zero at the wing tips.

$$\Gamma\left(\frac{b}{2}\right)=\Gamma\left(-\frac{b}{2}\right)=0 \qquad (12.52)$$

STANFORD
AERONAUTICS & ASTRONAUTICS

12.6 Elliptic lift distribution

$$\frac{\Gamma(y)}{\Gamma_0} = \left(1-\left(\frac{2y}{b}\right)^2\right)^{1/2} \tag{12.53}$$

$$\frac{d\Gamma(y)}{dy} = -\frac{4\Gamma_0}{b}\frac{\left(\frac{2y}{b}\right)}{\left(1-\left(\frac{2y}{b}\right)^2\right)^{1/2}} \tag{12.54}$$

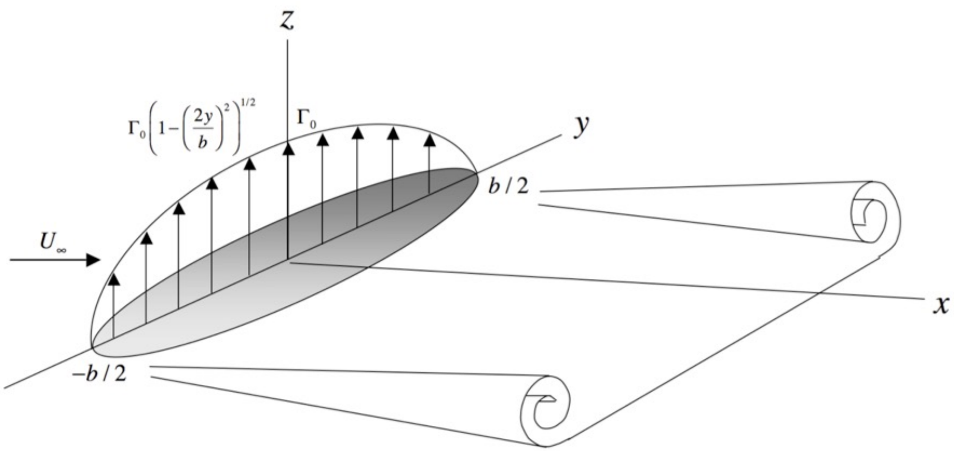

Figure 12.16 Elliptical load distribution

Total lift

$$L = \frac{1}{2}\rho U_\infty \Gamma_0 b \int_{-1}^{1}\left(1-\left(\frac{2y}{b}\right)^2\right)^{1/2} d\left(\frac{2y}{b}\right) = \rho U_\infty\left(\frac{\pi}{4}\Gamma_0 b\right) \tag{12.55}$$

Downwash velocity along the span of the lifting line

$$U_z(0,y,0)=\frac{\Gamma_0}{2\pi b}\int_{-1}^{1}\frac{\left(\frac{2y_0}{b}\right)}{\left(1-\left(\frac{2y_0}{b}\right)^2\right)^{1/2}}\left(\frac{1}{\frac{2y}{b}-\frac{2y_0}{b}}\right)d\left(\frac{2y_0}{b}\right) \qquad (12.56)$$

Let $2y/b = Sin(\theta)$ and $2y_0/b = Sin(\theta_0)$

$$U_z(0,\theta,0)=\frac{\Gamma_0}{2\pi b}\int_{-\pi/2}^{\pi/2}\frac{Sin(\theta_0)Cos(\theta_0)}{\left(1-Sin^2(\theta_0)\right)^{1/2}\left(Sin(\theta)-Sin(\theta_0)\right)}d\theta_0 \qquad (12.57)$$

$$U_z(0,\theta,0)=\frac{\Gamma_0}{2\pi b}\int_{-\pi/2}^{\pi/2}\frac{Sin(\theta_0)}{\left(Sin(\theta)-Sin(\theta_0)\right)}d\theta_0 \qquad (12.58)$$

$$U_z(0,\theta,0)=\frac{\Gamma_0}{2\pi b}\left(-\theta_0+Tan(\theta)Ln\left(\frac{Cos(\theta_0+\theta)}{Sin(\theta_0-\theta)}\right)\right)\Bigg|_{-\pi/2}^{\pi/2} \qquad (12.59)$$

For an elliptic lift distribution the downwash velocity is constant along the span

$$U_z(0,y,0)=-\frac{\Gamma_0}{2b} \qquad (12.60)$$

The downwash velocity everywhere is

$$U_z(x,y,z)=\frac{1}{4\pi}\int_{-b/2}^{b/2}\frac{d\Gamma}{dy_0}\times$$

$$\left(\frac{(y-y_0)\left((y-y_0)^2+z^2\right)^2-2(y-y_0)\left(x+\left(x^2+(y-y_0)^2+z^2\right)^{1/2}\right)\left(x^2+(y-y_0)^2+z^2\right)^{1/2}\left((y-y_0)^2+z^2\right)}{\left(x^2+(y-y_0)^2+z^2\right)^{1/2}\left(x+\left(x^2+(y-y_0)^2+z^2\right)^{1/2}\right)\left((y-y_0)^2+z^2\right)^2}\right)dy_0$$

(12.63)

STANFORD AERONAUTICS & ASTRONAUTICS

The downwash velocity on the centerline

$$U_z(x,0,0) = -\frac{1}{4\pi}\int_{-b/2}^{b/2}\frac{d\Gamma}{dy_0}\left(\frac{y_0^2 - 2\left(x+\left(x^2+y_0^2\right)^{1/2}\right)\left(x^2+y_0^2\right)^{1/2}}{y_0\left(x^2+y_0^2\right)^{1/2}\left(x+\left(x^2+y_0^2\right)^{1/2}\right)}\right)dy_0 \qquad (12.64)$$

$$U_z(x,0,0) = -\frac{\Gamma_0}{\pi b}\left(\frac{\pi}{2} + Sign(x)\times EllipticK\left(-\frac{1}{\left(\frac{2x}{b}\right)^2}\right)\right) \qquad (12.67)$$

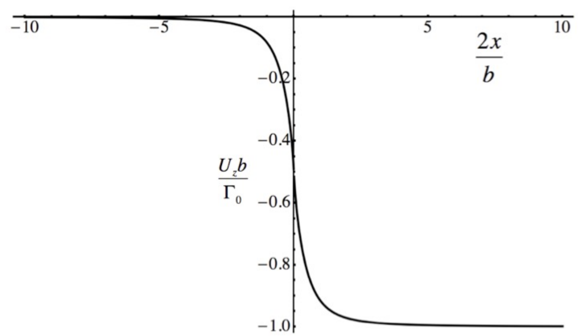

The downwash velocity in the far wake is twice the downwash at the lifting line.

Figure 12.17 Downwash induced along the x-axis by a continuous distribution of semi-infinite vortex lines of attached to the y-axis for the case of elliptic loading. Note the somewhat larger magnitude compared to two single vortex lines.

$$\lim_{x\to\infty} U_z(x,0,0) = -\frac{\Gamma_0}{b} \qquad (12.68)$$

STANFORD AERONAUTICS & ASTRONAUTICS

Solve the Prandtl equation for the chord distribution along the span.

$$\Gamma_0\left(1-\left(\frac{2y}{b}\right)^2\right)^{1/2}=\frac{1}{2}a_0(y)C(y)\left(U_\infty\alpha(y)-\frac{\Gamma_0}{2b}\right) \qquad (12.69)$$

There is an infinite variety of airfoils with different lift slopes $a_0(y)$, chord distributions $C(y)$ and angle of attack distributions $\alpha(y)$ that can generate an elliptic lift distribution. However if we assume the wing has the same cross-section geometry all along the span and that the angle of attack is constant as well, then a_0 and α are constant and (12.69) can be solved for the chord distribution.

For constant lift curve slope angle of attack and wing cross-section.

$$C(y)=C_0\left(1-\left(\frac{2y}{b}\right)^2\right)^{1/2} \qquad (12.70)$$

$$C_0=\frac{4b\Gamma_0}{\left(2bU_\infty a_0\alpha-a_0\Gamma_0\right)} \qquad (12.71)$$

Figure 12.18 British Spitfire showing elliptic planform wing. Note the wing is formed from two ellipses of different minor axis. This shifts the major axis and center of lift forward.

Republic P-47D Thunderbolt.

STANFORD AERONAUTICS & ASTRONAUTICS

Circulation at midspan.

$$\Gamma_0 = \frac{2bU_\infty a_0 C_0 \alpha}{a_0 C_0 + 4b} \tag{12.72}$$

Lift coefficient.

$$C_L = \frac{L}{\frac{1}{2}\rho U_\infty^2 S} = \frac{\pi}{2}\frac{\rho U_\infty b}{\rho U_\infty^2 S}\Gamma_0 = \pi\frac{b^2}{S}\left(\frac{1}{1+\frac{4b}{a_0 C_0}}\right)\alpha \tag{12.73}$$

Recall the aspect ratio.

$$A_R = \frac{b^2}{S} \tag{12.74}$$

$$S = \pi C_0 b / 4$$

$$C_L = \left(\frac{a_0 \alpha}{1+\frac{a_0}{\pi A_R}}\right) \tag{12.75}$$

STANFORD
AERONAUTICS &
ASTRONAUTICS

Effect of aspect ratio on the lift coefficient of an elliptic wing.

$$\frac{C_L}{2\pi\alpha} = \left(\frac{A_R}{2 + A_R}\right) \qquad (12.76)$$

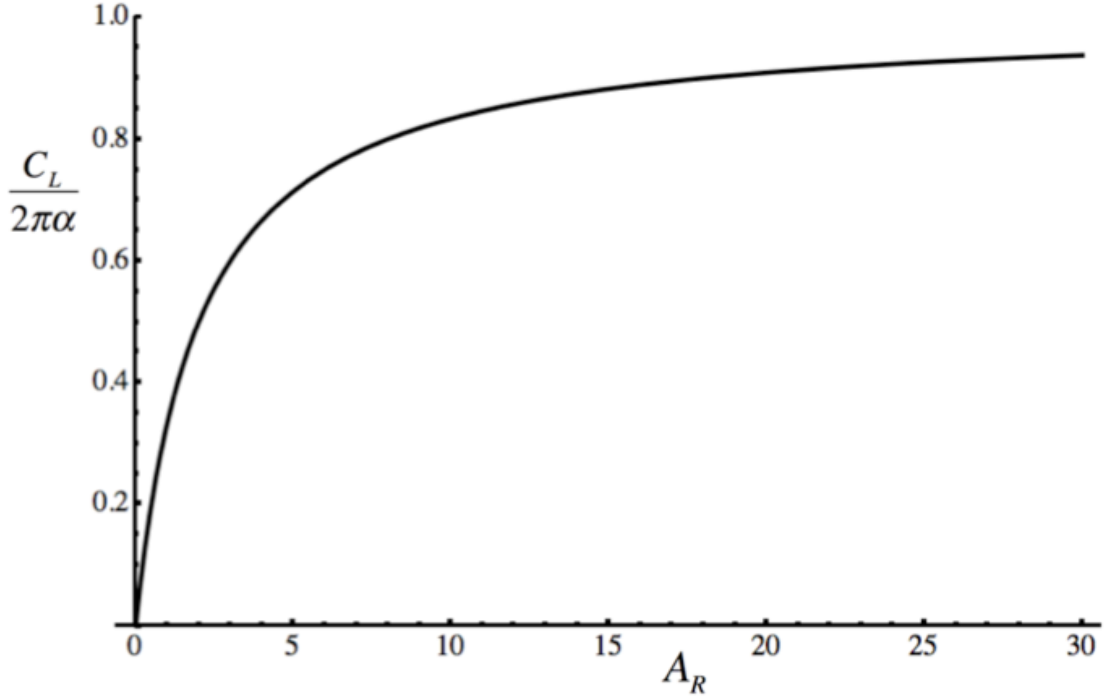

Figure 12.19 The effect of aspect ratio on the lift slope of a thin elliptical wing.

STANFORD AERONAUTICS & ASTRONAUTICS

12.7 Drag due to lift of an elliptic wing

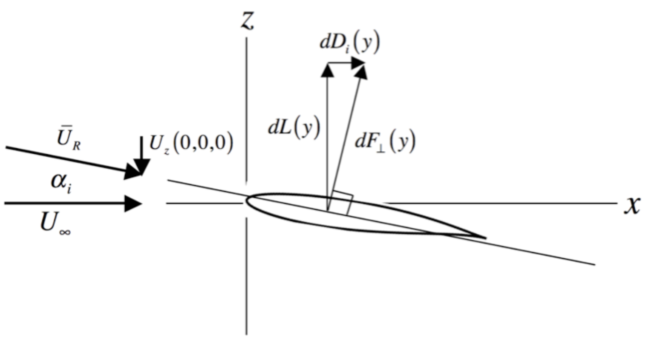

Fig 12.7 Differential forces on a section of a 3-D wing

$$L = F_\perp Cos(\alpha_i) = F_\perp \left(\frac{U_\infty}{\left(U_\infty^2 + U_z(0,0,0)^2\right)^{1/2}} \right) \qquad (12.77)$$

$$D_i = F_\perp Sin(-\alpha_i) = F_\perp \left(\frac{-U_z(0,0,0)}{\left(U_\infty^2 + U_z(0,0,0)^2\right)^{1/2}} \right) \qquad (12.78)$$

$$F_\perp = \left(\frac{\pi}{4}\right) \rho \left(U_\infty^2 + U_z(0,0,0)^2\right)^{1/2} \Gamma_0 b \qquad (12.79)$$

$$L = \left(\frac{\pi}{4}\right) \rho \left(U_\infty^2 + U_z(0,0,0)^2\right)^{1/2} \Gamma_0 b \left(\frac{U_\infty}{\left(U_\infty^2 + U_z(0,0,0)^2\right)^{1/2}} \right) = \left(\frac{\pi}{4}\right) \rho U_\infty \Gamma_0 b \qquad (12.80)$$

STANFORD AERONAUTICS & ASTRONAUTICS

Induced drag.

$$D_i = \left(\frac{\pi}{4}\right)\rho\left(U_\infty^2 + U_z(0,0,0)^2\right)^{1/2}\Gamma_0 b\left(\frac{-U_z(0,0,0)}{\left(U_\infty^2 + U_z(0,0,0)^2\right)^{1/2}}\right) = -\left(\frac{\pi}{4}\right)\rho U_z(0,0,0)\Gamma_0 b$$

Recall for an elliptic wing.

$$U_z(0,y,0) = -\frac{\Gamma_0}{2b} \qquad (12.81)$$

$$D_i = \left(\frac{\pi}{8}\right)\rho\Gamma_0^2 \qquad (12.82)$$

$$C_L = \frac{L}{\frac{1}{2}\rho U_\infty^2 S} = \frac{\pi}{2}\frac{\Gamma_0 b}{U_\infty S} \qquad (12.83)$$

$$C_{D_i} = \frac{D_i}{\frac{1}{2}\rho U_\infty^2 S} = \frac{\pi}{4}\frac{\Gamma_0^2}{U_\infty^2 S} \qquad (12.84)$$

Induced drag as a function of lift for an elliptic wing.

$$C_{D_i} = \frac{1}{\pi} C_L^2 \left(\frac{S}{b^2} \right) = \frac{1}{\pi} \frac{C_L^2}{A_R} \qquad (12.85)$$

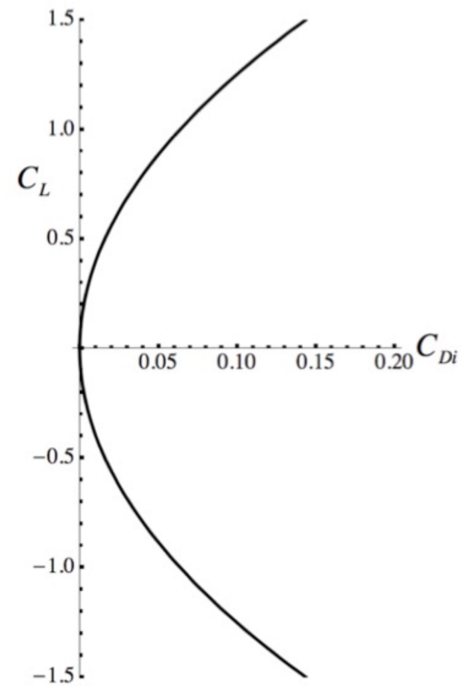

Figure 12.20 Lift to drag parabola for an elliptical wing with aspect ratio $A_R = 5$

Effect of aspect ratio on induced drag for an elliptic wing.

$$\frac{C_{D_i}}{4\pi\alpha^2} = A_R\left(\frac{1}{2+A_R}\right)^2 \tag{12.86}$$

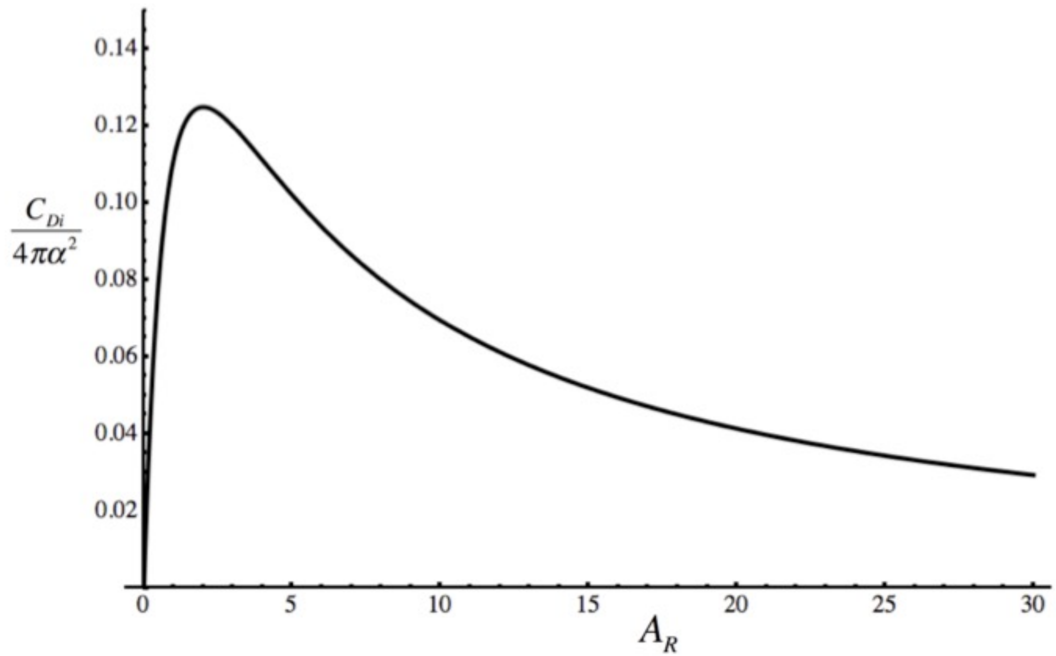

Figure 12.21 The effect of aspect ratio on the induced drag slope of a thin elliptical wing

STANFORD
AERONAUTICS &
ASTRONAUTICS

Effect of aspect ratio on lift to drag ratio for an elliptic wing.

$$\frac{C_L \alpha}{C_{D_i}} = 1 + \frac{A_R}{2} \tag{12.87}$$


Figure 12.22 Solar powered aircraft, left and U2 reconnaissance aircraft, right.

The unique feature of the elliptically loaded wing is that the downwash is constant along the span. This leads to simple analytical results for the lift, drag and shape of the wing. The really fortunate thing about these results is that they are not only elegant but important as well. The main reason is that all slender wings, whether they are rectangular, diamond or trapezoidal shaped can be viewed as modest variations away from the elliptic case. As for non-slender wings the elliptic case tells us how far from two-dimensional the wing behavior is as the aspect ratio becomes small.

Why aren't all wings designed to be elliptic?

1. At high angles of attack a wing with uniform cross section along the span and no twist will stall simultaneously all along the span causing sudden loss of aileron control. Increased chord at the wing tips helps maintain control authority.

2. Stall near the wing root is preferred and the wing can be twisted to reduce the angle of attack near the tips. This is called washout.

3. The induced drag penalty is relatively small even for relatively large deviations from an elliptical shape.

4. The compound curves involved in constructing an elliptic wing increase cost and complexity of manufacture.

12.8 General wing loadings

$$\Gamma(y)=\frac{1}{2}a_0(y)C(y)\left(U_\infty\alpha(y)-\frac{1}{4\pi}\int_{-b/2}^{b/2}\left(\frac{d\Gamma(y_0)}{dy_0}\right)\left(\frac{1}{(y-y_0)}\right)dy_0\right) \qquad (12.88)$$

Assume the downwash far downstream of the wing is twice the downwash at the wing at every spanwise point.

$$U_z(0,0,0)=\frac{U_z(\infty,0,0)}{2} \qquad (12.89)$$

$$U_z(0,y,0)=\lim_{x\to\infty}\frac{U_z(x,y,0)}{2} \qquad (12.90)$$

$$\Gamma(y)=\frac{1}{2}a_0(y)C(y)\left(U_\infty\alpha(y)+\lim_{x\to\infty}\frac{U_z(x,y,0)}{2}\right) \qquad (12.91)$$

Problem we would like to treat

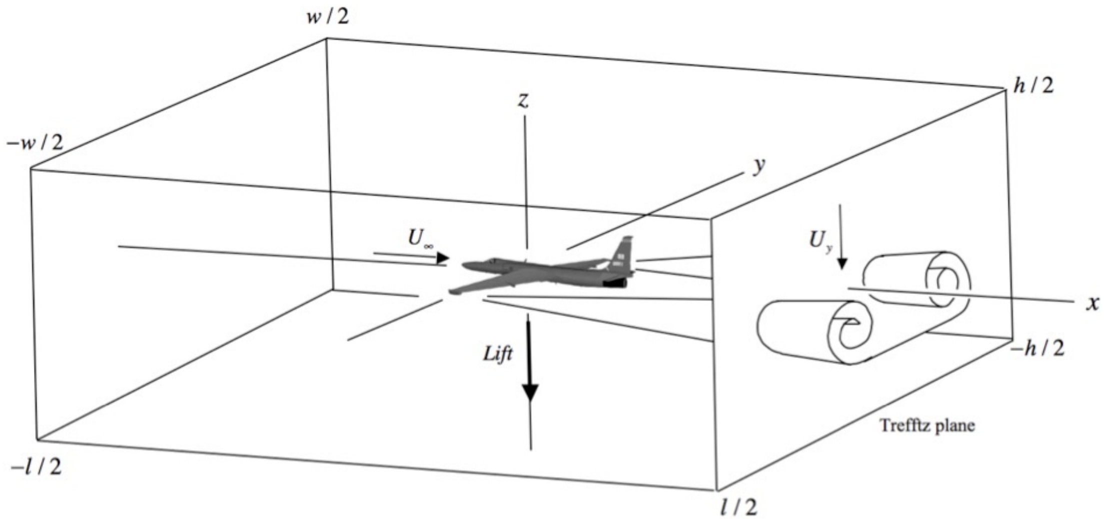

Figure 12.23 Trefftz plane intersecting the rolled up wake far behind an aircraft.

Problem we actually treat

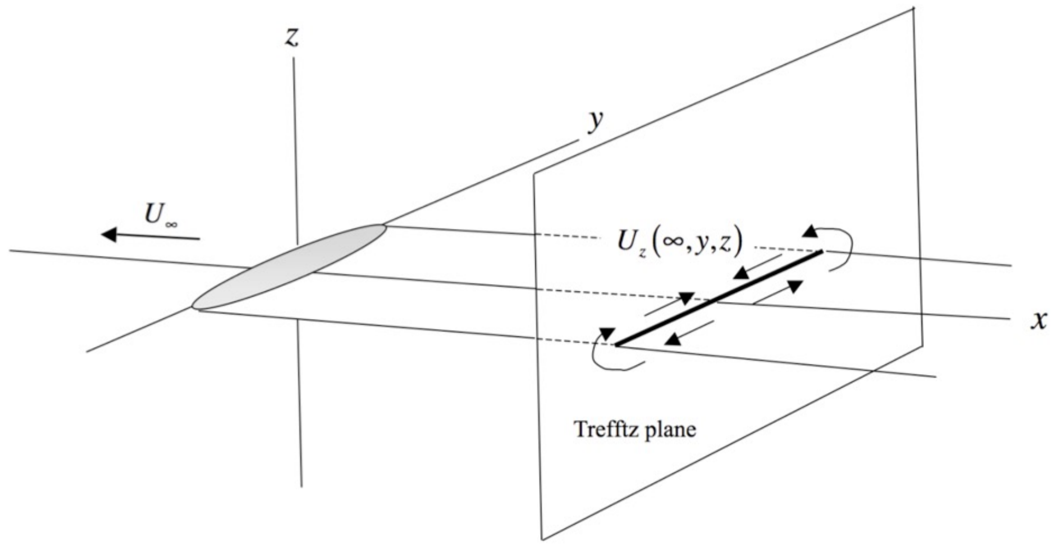

Figure 12.24 Trefftz plane intersecting the flat, straight vortex sheet from a wing

Far wake velocity field in the the (y,z) plane - the Trefftz plane

$$\lim_{x\to\infty} U_y(x,y,z) = \frac{1}{2\pi}\int_{-b/2}^{b/2} \frac{d\Gamma}{dy_0}\left(\frac{z}{\left((y-y_0)^2+z^2\right)}\right)dy_0$$

$$\lim_{x\to\infty} U_z(x,y,z) = -\frac{1}{2\pi}\int_{-b/2}^{b/2} \frac{d\Gamma}{dy_0}\left(\frac{(y-y_0)}{\left((y-y_0)^2+z^2\right)}\right)dy_0 \tag{12.92}$$

If the wing loading is elliptic

$$U_y(y,z) = -\frac{2\Gamma_0}{\pi b}\int_{-1}^{1} \frac{\left(\frac{2y_0}{b}\right)}{\left(1-\left(\frac{2y_0}{b}\right)^2\right)^{1/2}}\left(\frac{\left(\frac{2z}{b}\right)}{\left(\left(\frac{2y}{b}-\frac{2y_0}{b}\right)^2+\left(\frac{2z}{b}\right)^2\right)}\right)d\left(\frac{2y_0}{b}\right)$$

$$U_z(y,z) = \frac{2\Gamma_0}{\pi b}\int_{-1}^{1} \frac{\left(\frac{2y_0}{b}\right)}{\left(1-\left(\frac{2y_0}{b}\right)^2\right)^{1/2}}\left(\frac{\left(\frac{2y}{b}-\frac{2y_0}{b}\right)}{\left(\left(\frac{2y}{b}-\frac{2y_0}{b}\right)^2+\left(\frac{2z}{b}\right)^2\right)}\right)d\left(\frac{2y_0}{b}\right) \tag{12.93}$$

Let $2y/b = Cos(\theta)$ and $2y_0/b = Cos(\theta_0)$

$$U_y(y,z) = \frac{2\Gamma_0}{\pi b}\int_{-\pi}^{0}\left(\frac{Cos(\theta_0)\left(\frac{2z}{b}\right)}{\left(\left(Cos(\theta)-Cos(\theta_0)\right)^2+\left(\frac{2z}{b}\right)^2\right)}\right)d\theta_0$$

$$U_z(y,z) = -\frac{2\Gamma_0}{\pi b}\int_{-\pi}^{0}\left(\frac{Cos(\theta_0)\left(Cos(\theta)-Cos(\theta_0)\right)}{\left(\left(Cos(\theta)-Cos(\theta_0)\right)^2+\left(\frac{2z}{b}\right)^2\right)}\right)d\theta_0 \tag{12.94}$$

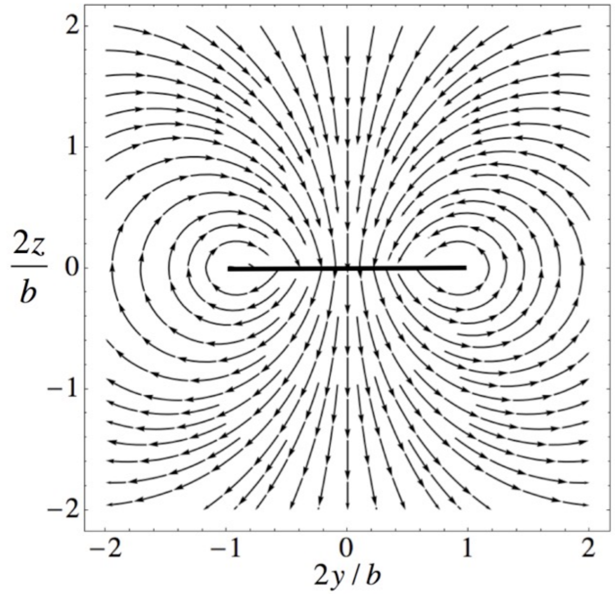

Figure 12.25 Flow in the Trefftz shown for an elliptically loaded wing.

Velocity field in the Trefftz plane for an elliptically loaded wing

$$u_y(y,0^+) = -u_y(y,0^-) \tag{12.95}$$

STANFORD AERONAUTICS & ASTRONAUTICS

The difference in spanwise velocity across the sheet is related to the circulation gradient in the y direction

$$\frac{d\Gamma(y)}{dy} = u_y\left(y,0^+\right) - u_y\left(y,0^-\right) = 2u_y\left(y,0^+\right) \qquad (12.96)$$

Trefftz plane potential

$$\lim_{x\to\infty} U_y\left(x,y,z\right) = u_y\left(y,z\right) = \frac{\partial\phi}{\partial y}$$

$$\lim_{x\to\infty} U_z\left(x,y,z\right) = u_z\left(y,z\right) = \frac{\partial\phi}{\partial z} \qquad (12.97)$$

$$\frac{d\Gamma(y)}{dy} = u_y\left(y,0^+\right) - u_y\left(y,0^-\right) = 2\frac{\partial\phi}{\partial y}\left(y,0^+\right) \qquad (12.98)$$

$$\Gamma(y) = 2\phi\left(y,0^+\right) \qquad \text{or} \qquad \Gamma(y) = -2\phi\left(y,0^-\right) \qquad (12.99)$$

The downwash velocity is continuous across the vortex sheet

$$\lim_{x\to\infty} U_z\left(x,y,0\right) = u_z\left(y,0\right) = \frac{\partial\phi}{\partial z}\left(y,0\right) \qquad (12.100)$$

Express the Prandtl equation in terms of the Trefftz plane potential.

$$\Gamma(y) = \frac{1}{2}a_0(y)C(y)\left(U_\infty\alpha(y) + \frac{1}{2}\frac{\partial\phi}{\partial z}\left(y,0\right)\right) \qquad (12.101)$$

Determine the Trefftz plane potential.

The problem boils down to determining the Trefftz plane potential $\phi(y,z)$. The problem formulation is as follows.

1) The potential satisfies Laplace's equation

$$\nabla^2\phi = \frac{\partial^2\phi}{\partial y^2} + \frac{\partial^2\phi}{\partial z^2} = 0 \tag{12.102}$$

2) The velocity goes to zero at large distances from the vortex sheet.

$$\lim_{\sqrt{y^2+z^2}\to\infty} \nabla\phi \to 0 \tag{12.103}$$

3) The velocity potential is an odd function of z.

$$\phi(y,z) = -\phi(y,-z) \tag{12.104}$$

The condition (12.104) comes from

$$\phi\left(y,0^{+}\right)=-\phi\left(y,0^{-}\right) \quad \text{for} \quad -b/2<y<b/2 \tag{12.105}$$

and

$$\phi(y,0)=0 \qquad \text{for} \qquad y<-b/2 \qquad \text{and} \qquad y>b/2 \tag{12.106}$$

In addition, at the end points of the vortex sheet

$$\phi\left(-\frac{b}{2},0\right)=\phi\left(\frac{b}{2},0\right)=0 \tag{12.107}$$

4) The Prandtl equation provides the boundary condition

$$2\phi\left(y,0^{+}\right)=\frac{1}{2}a_{0}(y)C(y)\left(U_{\infty}\alpha(y)+\frac{1}{2}\frac{\partial\phi}{\partial z}(y,0)\right) \quad \text{for} \quad -b/2<y<b/2 \tag{12.108}$$

where (12.99) has been used.

Use complex analysis to solve the problem.

$$\xi = y + iz = \rho e^{i\vartheta} = \rho\left(Cos\left(\vartheta\right) + iSin\left(\vartheta\right)\right) \tag{12.109}$$

$$F\left(\xi\right) = \phi\left(y,z\right) + i\psi\left(y,z\right) \tag{12.110}$$

$$u_y\left(y,z\right) = \frac{\partial\phi}{\partial y} \qquad u_z\left(y,z\right) = \frac{\partial\phi}{\partial z} \tag{12.111}$$

$$u_y\left(y,z\right) = \frac{\partial\psi}{\partial z} \qquad u_z\left(y,z\right) = -\frac{\partial\psi}{\partial y} \tag{12.112}$$

$$\frac{\partial\phi}{\partial y} = \frac{\partial\psi}{\partial z} \qquad \frac{\partial\phi}{\partial z} = -\frac{\partial\psi}{\partial y} \tag{12.113}$$

Complex velocity.

The derivative of an analytic function is independent of the path in the complex plane along which $\Delta\xi \to 0$. Therefore the complex velocity can be either

$$W(\xi) = \frac{dF}{d\xi} = \frac{dF}{dy}\left(\frac{1}{d\xi / dy}\right) = \frac{\partial \phi(y,z)}{\partial y} + i\frac{\partial \psi(y,z)}{\partial y} = u_y(y,z) - iu_z(y,z) \qquad (12.114)$$

or

$$W(\xi) = \frac{dF}{d\xi} = \frac{dF}{dz}\left(\frac{1}{d\xi / dz}\right) = -i\frac{\partial \phi(y,z)}{\partial z} + \frac{\partial \psi(y,z)}{\partial z} = u_y(y,z) - iu_z(y,z) \qquad (12.115)$$

Either derivative generates the same velocity field.

Joukowsky transformation in reverse

$$\xi(\eta) = \eta + \frac{(b/4)^2}{\eta} \qquad (12.116)$$

$$\eta = p + iq = re^{i\theta} = r\left(Cos(\theta) + iSin(\theta)\right) \qquad (12.117)$$

$$r = \sqrt{p^2 + q^2} \qquad \theta = ArcTan\left(\frac{q}{p}\right) \qquad (12.118)$$

$$\eta = \frac{\xi}{2} \pm \frac{1}{2}\sqrt{\xi^2 - \left(\frac{b}{2}\right)^2} \qquad (12.119)$$

$$y = p\left(1 + \left(\frac{b}{4}\right)^2 \frac{1}{p^2 + q^2}\right) \qquad z = q\left(1 - \left(\frac{b}{4}\right)^2 \frac{1}{p^2 + q^2}\right) \qquad (12.120)$$

$$y = Cos(\theta)\left(r + \left(\frac{b}{4}\right)^2 \frac{1}{r}\right) \qquad z = Sin(\theta)\left(r - \left(\frac{b}{4}\right)^2 \frac{1}{r}\right) \tag{12.121}$$

$$\rho = \sqrt{\frac{b^4}{16r^2} + r^2 + \frac{b^2}{2}Cos(2\theta)} \qquad \vartheta = ArcTan\left(\frac{r - \dfrac{b^2}{4r}}{r + \dfrac{b^2}{4r}}Tan(\theta)\right) \tag{12.122}$$

The mapping (12.116) takes the line $z = 0$, $-b/2 < y < b/2$ in the ξ plane to the circle

$$\eta_{Sheet} = \left(\frac{b}{4}\right)\left(Cos(\theta) + iSin(\theta)\right) = \left(\frac{b}{4}\right)e^{i\theta} \tag{12.123}$$

STANFORD
AERONAUTICS & ASTRONAUTICS

Map the vortex sheet in the Trefftz plane to a circle

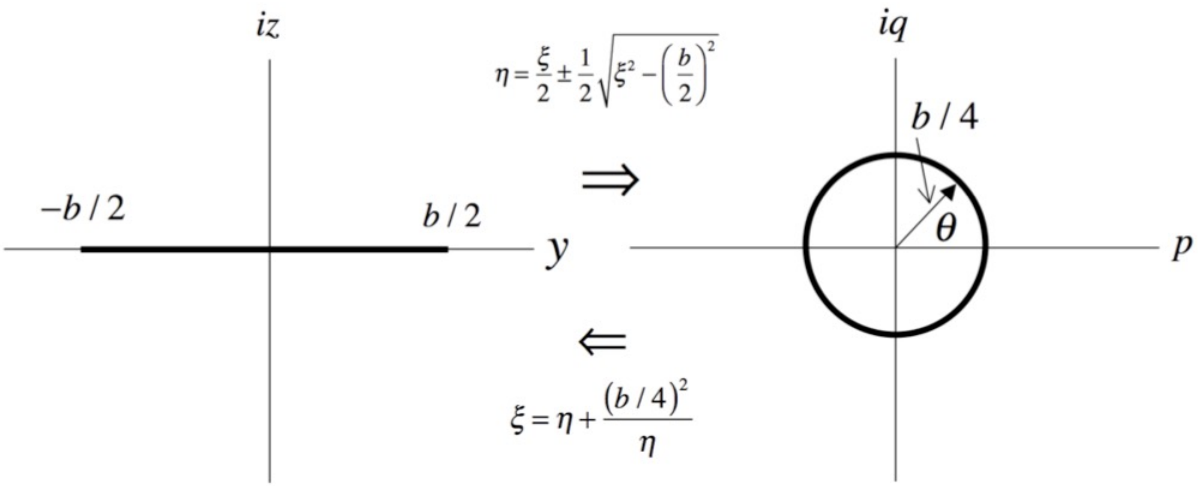

Figure 12.26 Mapping the vortex sheet to a circle

$$G(\eta) = \varphi(r,\theta) + i\zeta(r,\theta) \qquad (12.124)$$

$$G(\eta) = F(\xi(\eta)) \qquad (12.125)$$

$$F(\xi) = G(\eta(\xi)) \qquad (12.126)$$

$$\phi(y,z) = \varphi(r(y,z),\theta(y,z)) \qquad (12.127)$$

STANFORD
AERONAUTICS &
ASTRONAUTICS

Assume the complex potential in the eta plane is of the form

$$G(\eta)=\sum_{n=1}^{\infty}\left(\frac{b_n+ia_n}{\eta^n}\right) \tag{12.128}$$

$$G(\eta)=\sum_{n=1}^{\infty}\left(\frac{\left(b_nCos(n\theta)+a_nSin(n\theta)\right)+i\left(a_nCos(n\theta)-b_nSin(n\theta)\right)}{r^n}\right) \tag{12.129}$$

$$\varphi(r,\theta)=\sum_{n=1}^{\infty}\left(\frac{\left(b_nCos(n\theta)+a_nSin(n\theta)\right)}{r^n}\right) \tag{12.130}$$

$$\varphi(r,\theta)=-\varphi(r,-\theta)\quad \text{for}\quad r\geq b/4 \tag{12.131}$$

$$\varphi(r,0)=\varphi(r,\pi)\quad \text{for}\quad r>b/4 \tag{12.132}$$

Coefficients of the symmetric terms in 12.130 must all be zero

$$\varphi(r,\theta)=\sum_{n=1}^{\infty}\frac{a_nSin(n\theta)}{r^n} \tag{12.133}$$

STANFORD
AERONAUTICS &
ASTRONAUTICS

Complex potential in the eta plane

$$G(\eta)=i\sum_{n=1}^{\infty}\left(\frac{a_n}{\eta^n}\right) \tag{12.134}$$

$$\phi(y,z)=\varphi\big(r(y,z),\theta(y,z)\big)=\sum_{n=1}^{\infty}\frac{a_n Sin\big(n\theta(y,z)\big)}{r(y,z)^n} \tag{12.135}$$

Complex potential in the xi plane

$$W(\xi)=u_y(y,z)-iu_z(y,z)=\frac{dF}{d\xi}=\frac{dG}{d\eta}\left(\frac{1}{d\xi/d\eta}\right) \tag{12.136}$$

$$u_y(y,z)-iu_z(y,z)=-i\sum_{n=1}^{\infty}\left(\frac{na_n}{\eta^{n+1}}\right)\left(\frac{\eta^2}{\eta^2-\left(\frac{b}{4}\right)^2}\right) \tag{12.137}$$

Complex velocity in the xi plane

$$u_y(y,z)-iu_z(y,z)=-i\sum_{n=1}^{\infty}\left(\frac{na_n e^{-n\theta}}{r^{n+1}}\right)\left(\frac{r^2}{r^2e^{i\theta}-\left(\frac{b}{4}\right)^2 e^{-i\theta}}\right) \tag{12.138}$$

STANFORD
AERONAUTICS & ASTRONAUTICS

$$u_y(y,z)-iu_z(y,z)=-i\sum_{n=1}^{\infty}\left(\frac{na_n e^{-in\theta}}{r^{n+1}}\right)\left(\frac{r^2}{r^2e^{i\theta}-\left(\frac{b}{4}\right)^2 e^{-i\theta}}\right)\left(\frac{r^2e^{-i\theta}-\left(\frac{b}{4}\right)^2 e^{i\theta}}{r^2e^{-i\theta}-\left(\frac{b}{4}\right)^2 e^{i\theta}}\right)=$$

$$-\sum_{n=1}^{\infty}\left(\frac{na_n\left(\begin{array}{l}\left(\left(r^2+\left(\frac{b}{4}\right)^2\right)Cos(n\theta)Sin(\theta)+\left(r^2-\left(\frac{b}{4}\right)^2\right)Sin(n\theta)Cos(\theta)\right)+\\ i\left(\left(r^2-\left(\frac{b}{4}\right)^2\right)Cos(n\theta)Cos(\theta)-\left(r^2+\left(\frac{b}{4}\right)^2\right)Sin(n\theta)Sin(\theta)\right)\end{array}\right)}{r^{n-1}\left(r^4+\left(\frac{b}{4}\right)^4-2\left(\frac{b}{4}\right)^2r^2Cos(2\theta)\right)}\right)$$

(12.139)

STANFORD
AERONAUTICS & ASTRONAUTICS

Separate the complex velocity into real and imaginary parts

$$u_y(y,z) - iu_z(y,z) = \frac{\partial\phi(y,z)}{\partial y} - i\frac{\partial\phi(y,z)}{\partial z} =$$

$$-\sum_{n=1}^{\infty}\left(\frac{na_n\left(\left(\left(r^2+\left(\frac{b}{4}\right)^2\right)Cos(n\theta)Sin(\theta)+\left(r^2-\left(\frac{b}{4}\right)^2\right)Sin(n\theta)Cos(\theta)\right)\right)}{r^{n-1}\left(r^4+\left(\frac{b}{4}\right)^4-2\left(\frac{b}{4}\right)^2 r^2Cos(2\theta)\right)}\right)$$

$$-i\sum_{n=1}^{\infty}\left(\frac{na_n\left(\left(\left(r^2-\left(\frac{b}{4}\right)^2\right)Cos(n\theta)Cos(\theta)-\left(r^2+\left(\frac{b}{4}\right)^2\right)Sin(n\theta)Sin(\theta)\right)\right)}{r^{n-1}\left(r^4+\left(\frac{b}{4}\right)^4-2\left(\frac{b}{4}\right)^2 r^2Cos(2\theta)\right)}\right) \qquad (12.140)$$

Downwash velocity in the xi plane

$$\frac{\partial\phi(y,z)}{\partial z} = \sum_{n=1}^{\infty}\left(\frac{na_n\left(\left(\left(r^2-\left(\frac{b}{4}\right)^2\right)Cos(n\theta)Cos(\theta)-\left(r^2+\left(\frac{b}{4}\right)^2\right)Sin(n\theta)Sin(\theta)\right)\right)}{r^{n-1}\left(r^4+\left(\frac{b}{4}\right)^4-2\left(\frac{b}{4}\right)^2 r^2 Cos(2\theta)\right)}\right) \qquad (12.141)$$

$$\left.\frac{\partial\phi(y,z)}{\partial z}\right|_{z=0} = \sum_{n=1}^{\infty}\left.\left(\frac{na_n\left(\left(\left(r^2-\left(\frac{b}{4}\right)^2\right)Cos(n\theta)Cos(\theta)-\left(r^2+\left(\frac{b}{4}\right)^2\right)Sin(n\theta)Sin(\theta)\right)\right)}{r^{n-1}\left(r^4+\left(\frac{b}{4}\right)^4-2\left(\frac{b}{4}\right)^2 r^2 Cos(2\theta)\right)}\right)\right|_{r=b/4} =$$

$$-\sum_{n=1}^{\infty}\left(\frac{na_n Sin(n\theta)Sin(\theta)}{\left(\frac{b}{4}\right)^{n+1}\left(1-Cos(2\theta)\right)}\right) = -\sum_{n=1}^{\infty}\left(\frac{na_n}{2\left(\frac{b}{4}\right)^{n+1}}\frac{Sin(n\theta)}{Sin(\theta)}\right) \qquad (12.142)$$

STANFORD
AERONAUTICS & ASTRONAUTICS

Downwash velocity in the xi plane at z=0

$$\left.\frac{\partial\phi(y,z)}{\partial z}\right|_{z=0} = -\sum_{n=1}^{\infty}\left(\frac{na_n}{2\left(\frac{b}{4}\right)^{n+1}}\frac{Sin(n\theta)}{Sin(\theta)}\right) \tag{12.143}$$

Potential in the xi plane at z=0

$$\left.\phi(y,z)\right|_{z=0^+} = \left.\sum_{n=1}^{\infty}\frac{a_n Sin(n\theta(y,z))}{r(y,z)^n}\right|_{r=b/4} = \sum_{n=1}^{\infty}\frac{a_n Sin(n\theta)}{\left(\frac{b}{4}\right)^n} \tag{12.144}$$

Substitute 12.143 and 12.144 into the Prandtl equation and rearrange

$$\frac{\phi(y,0^+)}{U_\infty b} - \frac{1}{8}a_0(y)\left(\frac{C(y)}{b}\right)\frac{1}{U_\infty}\frac{\partial\phi}{\partial z}(y,0) = \frac{1}{4}a_0(y)\left(\frac{C(y)}{b}\right)\alpha(y) \quad \text{for} \quad -\frac{b}{2} < y < \frac{b}{2}$$

(12.145)

$$\frac{\phi\left(y,0^{+}\right)}{U_{\infty}b}-\frac{1}{8}a_{0}(y)\left(\frac{C(y)}{b}\right)\frac{1}{U_{\infty}}\frac{\partial\phi}{\partial z}(y,0)=\frac{1}{4}a_{0}(y)\left(\frac{C(y)}{b}\right)\alpha(y)$$

$$\frac{1}{U_{\infty}b}\sum_{n=1}^{\infty}\frac{a_{n}Sin(n\theta)}{\left(\frac{b}{4}\right)^{n}}+\frac{1}{8}a_{0}(y)\left(\frac{C(y)}{b}\right)\frac{1}{U_{\infty}}\sum_{n=1}^{\infty}\left(\frac{na_{n}}{2\left(\frac{b}{4}\right)^{n+1}}\frac{Sin(n\theta)}{Sin(\theta)}\right)=\frac{1}{4}a_{0}(y)\left(\frac{C(y)}{b}\right)\alpha(y)$$

$$\sum_{n=1}^{\infty}\frac{a_{n}Sin(n\theta)}{U_{\infty}b\left(\frac{b}{4}\right)^{n}}\left(Sin(\theta)+\frac{na_{0}(y)C(y)}{4b}\right)=a_{0}(y)\left(\frac{C(y)}{4b}\right)\alpha(y)Sin(\theta)$$

$$\sum_{n=1}^{\infty}\left(\frac{a_{n}Sin(n\theta)}{U_{\infty}b\left(\frac{b}{4}\right)^{n}}\left(Sin(\theta)+\frac{na_{0}(y)C(y)}{4b}\right)\right)=a_{0}(y)\left(\frac{C(y)}{4b}\right)\alpha(y)Sin(\theta)$$

(12.146)

STANFORD AERONAUTICS & ASTRONAUTICS

Solution for the potential

$$\phi(y,z)=\sum_{n=1}^{\infty}\frac{a_n Sin\left(n\theta(y,z)\right)}{r(y,z)^n} \qquad (12.147)$$

Evaluate the Prandtl equation on the vortex sheet

$$\sum_{n=1}^{\infty}\left(\frac{a_n Sin(n\theta)}{U_\infty b\left(\frac{b}{4}\right)^n}\left(Sin(\theta)+n\frac{a_0(y)C(y)}{4b}\right)\right)=\left(\frac{a_0(y)C(y)}{4b}\right)\alpha(y)Sin(\theta) \qquad (12.148)$$

Coefficients are determined from

$$\sum_{n=1}^{\infty}\left(\frac{a_n Sin(n\theta)}{U_\infty b\left(\frac{b}{4}\right)^n}\left(Sin(\theta)+\frac{na_0\left(\frac{b}{2}Cos(\theta)\right)C\left(\frac{b}{2}Cos(\theta)\right)}{4b}\right)\right)= \qquad (12.149)$$

$$a_0(y)\left(\frac{C\left(\frac{b}{2}Cos(\theta)\right)}{4b}\right)\alpha\left(\frac{b}{2}Cos(\theta)\right)Sin(\theta)$$

Check against the case of an elliptic wing

$$C(y) = C_0\left(1-\left(\frac{2y}{b}\right)^2\right)^{1/2} = C_0 Sin(\theta) \qquad (12.150)$$

$$\sum_{n=1}^{\infty}\left(\frac{a_n Sin(n\theta)}{U_\infty b\left(\frac{b}{4}\right)^n}\left(Sin(\theta)+\frac{na_0(y)C(y)}{4b}\right)\right) = a_0(y)\left(\frac{C(y)}{4b}\right)\alpha(y)Sin(\theta)$$

$$C(y) = C_0 Sin(\theta)$$

$$\sum_{n=1}^{\infty}\left(\frac{a_n Sin(n\theta)}{U_\infty b\left(\frac{b}{4}\right)^n}\left(Sin(\theta)+\frac{na_0(y)C_0 Sin(\theta)}{4b}\right)\right) = a_0(y)\left(\frac{C_0 Sin(\theta)}{4b}\right)\alpha(y)Sin(\theta)$$

$$\sum_{n=1}^{\infty}\left(\frac{a_n Sin(n\theta)}{U_\infty b\left(\frac{b}{4}\right)^n}\left(1+\frac{na_0 C_0}{4b}\right)\right) = a_0\left(\frac{C_0 Sin(\theta)}{4b}\right)\alpha \qquad (12.151)$$

$$a_n = 0, n = 2,3,\ldots$$

$$1 = \frac{a_0}{a_1}\left(\frac{C_0}{4}\right)U_\infty\left(\frac{b}{4}\right)\alpha - \frac{a_0 C_0}{4b} = C_0\left(\frac{a_0}{4a_1}U_\infty\left(\frac{b}{4}\right)\alpha - \frac{a_0}{4b}\right)$$

Centerline chord

$$C_0 = \frac{4b}{a_0\left(\frac{U_\infty}{a_1}\left(\frac{b}{2}\right)^2\alpha - 1\right)}$$

Compare to the equation for the centerline chord that we derived when we established the theory of an elliptic wing (12.71)

$$C_0 = \frac{4b\Gamma_0}{\left(2bU_\infty a_0\alpha - a_0\Gamma_0\right)} = \frac{4b}{a_0\left(\dfrac{2bU_\infty}{\Gamma_0}\alpha - 1\right)} =$$

$$C_0 = \frac{4b}{a_0\left(\dfrac{U_\infty}{\left(\Gamma_0 b/8\right)}\left(\dfrac{b}{2}\right)^2\alpha - 1\right)} \qquad (12.152)$$

Where we choose

$$a_1 = \frac{\Gamma_0 b}{8} \qquad (12.153)$$

$$\left.\frac{\partial\phi(y,z)}{\partial z}\right|_{z=0} = -\left(\frac{8a_1}{b^2}\right)$$

$$a_1 = \frac{\Gamma_0 b}{8} \qquad (12.154)$$

The downwash also checks

$$\left.\frac{\partial\phi(y,z)}{\partial z}\right|_{z=0} = -\left(\frac{\Gamma_0}{b}\right)$$

STANFORD
AERONAUTICS & ASTRONAUTICS

That is some reassurance that (12.148) is correct. Since $y = bCos(\theta)/2$ we can let $C(y) = C(\theta)$, $a_0(y) = a_0(\theta)$ and $\alpha(y) = \alpha(\theta)$. The Prandtl equation becomes

$$\sum_{n=1}^{\infty}\left(\frac{a_n Sin(n\theta)}{U_\infty b\left(\frac{b}{4}\right)^n}\left(Sin(\theta) + n\frac{a_0(\theta)C(\theta)}{4b}\right)\right) = \left(\frac{a_0(\theta)C(\theta)}{4b}\right)\alpha(\theta)Sin(\theta) \quad (12.155)$$

The circulation and downwash on a general wing shape

$$\frac{\Gamma(y)}{2U_\infty b} = \sum_{n=1}^{\infty} A_n Sin(n\theta) \quad (12.156)$$

$$\frac{U_z(0,y,0)}{U_\infty} = -\sum_{n=1}^{\infty}\left(nA_n \frac{Sin(n\theta)}{Sin(\theta)}\right) \quad (12.157)$$

where

$$A_n = \frac{a_n}{U_\infty b\left(\frac{b}{4}\right)^n} \quad (12.158)$$

12.9 Forces on a general wing

Lift

$$dL(y) = \rho U_\infty \Gamma(y)dy \qquad (12.159)$$

Induced drag

$$dD_i(y) = \rho U_z(0,y,0)\Gamma(y)dy \qquad (12.160)$$

$$y = \frac{b}{2}Cos(\theta) \quad \text{and} \quad dy = -\frac{b}{2}Sin(\theta)d\theta \qquad (12.161)$$

The range on y is $-b/2 < y < b/2$ and $-\pi < \theta < 0$.

$$dL(y) = \rho U_\infty^2 b^2 \sum_{n=1}^{\infty} A_n Sin(n\theta) Sin(\theta)d\theta \qquad (12.162)$$

$$dD_i(y) = \rho U_\infty^2 b^2 \left(\sum_{n=1}^{\infty} (nA_n Sin(n\theta)) \sum_{m=1}^{\infty} A_m Sin(m\theta) \right) d\theta \qquad (12.163)$$

$$L = \rho U_\infty^2 b^2 \sum_{n=1}^{\infty} A_n \int_{-\pi}^{0} Sin(n\theta) Sin(\theta)\, d\theta \qquad (12.164)$$

$$D_i = \rho U_\infty^2 b^2 \sum_{n=1}^{\infty} \sum_{m=1}^{\infty} n A_n A_m \int_{-\pi}^{0} Sin(n\theta) Sin(m\theta)\, d\theta \qquad (12.165)$$

$$\int_{-\pi}^{0} Sin(n\theta) Sin(m\theta) d\theta = 0 \text{ if } n \neq m \;,\; \int_{-\pi}^{0} Sin(n\theta) Sin(m\theta) d\theta = \frac{\pi}{2} \text{ if } n = m \qquad (12.166)$$

Lift only depends on the first coefficient in the series

$$L = \frac{\pi}{2} \rho U_\infty^2 b^2 A_1 \qquad (12.167)$$

Induced drag depends on all coefficients in the series

$$D_i = \frac{\pi}{2} \rho U_\infty^2 b^2 \sum_{n=1}^{\infty} n A_n^2 \qquad (12.168)$$

Roll moment

$$M_x = M_{Roll} = \rho U_\infty \int_{-b/2}^{b/2} y\Gamma(y)dy = -\frac{1}{2}\rho U_\infty^2 b^3 \sum_{n=1}^{\infty} A_n \int_{-\pi}^{0} Sin(n\theta)Cos(\theta)Sin(\theta)d\theta \quad (12.169)$$

$$\int_{-\pi}^{0} Sin(n\theta)Cos(\theta)Sin(\theta)d\theta = 0 \quad \text{all} \quad n \neq 2\,, \quad \int_{-\pi}^{0} Sin(2\theta)Cos(\theta)Sin(\theta)d\theta = \frac{\pi}{4}$$

(12.170)

Roll moment only depends on A_2

$$M_x = M_{Roll} = \rho U_\infty \int_{-b/2}^{b/2} y\Gamma(y)dy = -\frac{\pi}{8}\rho U_\infty^2 b^3 A_2 \quad (12.171)$$

Yaw moment

$$M_z = M_{Yaw} = -\int_{-b/2}^{b/2} y\, dD_i(y) = \rho \int_{-b/2}^{b/2} yU_z(0,y,0)\Gamma(y)dy \quad (12.172)$$

$$M_z = M_{Yaw} = \rho \int_{-b/2}^{b/2} yU_z(0,y,0)\Gamma(y)dy =$$

$$\frac{1}{2}\rho U_\infty^2 b^3 \sum_{n=1}^{\infty}\sum_{m=1}^{\infty} nA_n A_m \int_{-\pi}^{0} Sin(n\theta)Sin(m\theta)Sin(\theta)Cos(\theta)d\theta \quad (12.173)$$

Yaw moment depends on all coefficients

$$M_z = M_{Yaw} = \frac{\pi}{8}\rho U_\infty^2 b^3 \sum_{n=1}^{\infty}(2n+1)A_n A_{n+1} \quad (12.175)$$

STANFORD AERONAUTICS & ASTRONAUTICS

Force and moment coefficients

$$
\begin{aligned}
C_L &= \frac{L}{\frac{1}{2}\rho U_\infty^2 S} = \pi\left(\frac{b^2}{S}\right)A_1 = (\pi A_R)A_1 \\
C_{D_i} &= \frac{D_i}{\frac{1}{2}\rho U_\infty^2 S} = \pi\left(\frac{b^2}{S}\right)\sum_{n=1}^{\infty} nA_n^2 = (\pi A_R)\sum_{n=1}^{\infty} nA_n^2 \\
C_{MRoll} &= \frac{M_x}{\frac{1}{2}\rho U_\infty^2 Sb} = -\frac{\pi}{4}\left(\frac{b^2}{S}\right)A_2 = -\left(\frac{\pi}{4}A_R\right)A_2 \\
C_{MYaw} &= \frac{M_z}{\frac{1}{2}\rho U_\infty^2 Sb} = \frac{\pi}{4}\left(\frac{b^2}{S}\right)\sum_{n=1}^{\infty}(2n+1)A_nA_{n+1} = \left(\frac{\pi}{4}A_R\right)\sum_{n=1}^{\infty}(2n+1)A_nA_{n+1}
\end{aligned}
\qquad (12.176)
$$

Pitching moment coefficient is determined from 2-D wing profile analysis - Chapter 11

Recall the pitching moment from 2D wing theory

Pitching moment due to camber

$$C_M = \frac{M}{\frac{1}{2}\rho U_\infty^2 C^2} = \frac{1}{2U_\infty}\int_0^\pi \gamma(\theta)\left(1+Cos(\theta)\right)Sin(\theta)\,d\theta = \quad . \qquad (11.117)$$

$$-\frac{\pi}{4}\left(2B_0 + B_1\right) - \frac{\pi}{4}\left(B_1 + B_2\right)$$

The moment coefficient due to camber can be thought of as a pure moment or couple about the leading edge plus a moment due to lift acting at the 1/4 chord point.

$$C_M = \frac{C_L}{4} - \frac{\pi}{4}\left(B_1 + B_2\right). \qquad (11.118)$$

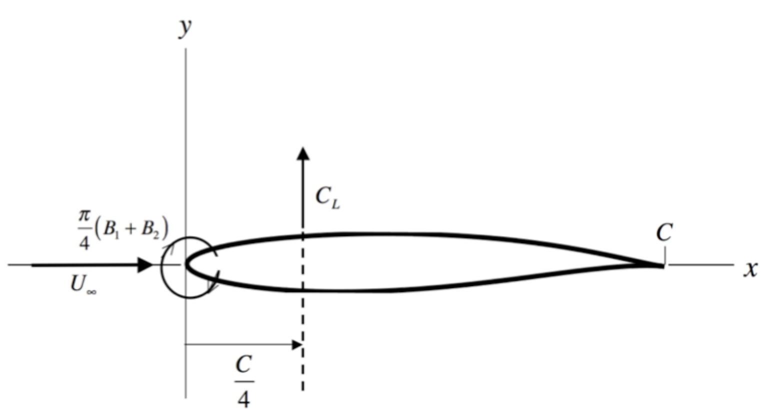

Figure 11.16 Forces and moments on a thin cambered airfoil at zero angle of attack.

The angle-of-attack problem

Finally we look at the incompressible potential flow past a flat plate at a small angle of attack illustrated below. The source is modeled as a distribution of vortices as in the camber problem.

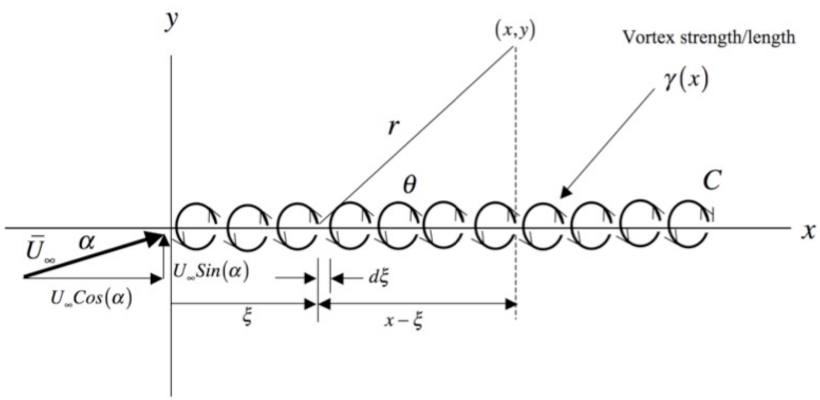

Figure 11.17 Distribution of vortices generating lift on a flat plate at angle-of-attack α .

$$\gamma(\theta) = 2U_{\infty}\alpha\left(\frac{1-Cos(\theta)}{Sin(\theta)}\right). \qquad (11.122)$$

$$C_L = 2\pi\alpha$$

$$C_M = \frac{\pi}{2}\alpha \qquad (11.123)$$

Pitching moment due to angle-of-attack

$$C_M = \frac{C_L}{4}$$

In 3D the effect of downwash on the pitching moment is felt through the modified angle-of-attack

Potential flow for a flat plate at an angle of attack in low speed flow.

$$\gamma(\theta) = 2U_{\infty}\alpha\left(\frac{1 - Cos(\theta)}{Sin(\theta)}\right). \qquad (11.122)$$

$$C_L = 2\pi\alpha$$
$$C_M = \frac{\pi}{2}\alpha \, . \qquad (11.123)$$

Pitching moment due to camber

STANFORD
AERONAUTICS &
ASTRONAUTICS

12.10 Minimum induced drag wing

The coefficients in (12.176) depend on the distributions of $a_0(y), C(y), \alpha(y)$ along the span of the wing. The lift only depends on the the first coefficient. The drag depends on a sum of squares of all the coefficients. Clearly the lowest drag occurs when $A_n = 0$ for all $n > 1$. In this case the circulation (12.156) becomes

$$\Gamma(y) = 2U_\infty b A_1 Sin(\theta) = 2U_\infty b A_1 \left(1 - \left(\frac{2y}{b}\right)^2\right)^{1/2} = 8\frac{a_1}{b}\left(1 - \left(\frac{2y}{b}\right)^2\right)^{1/2} \qquad (12.177)$$

Recall (12.153), $a_1 = \Gamma_0 b / 8$. Now

$$\Gamma(y) = \Gamma_0 \left(1 - \left(\frac{2y}{b}\right)^2\right)^{1/2} \qquad (12.178)$$

Minimum induced drag occurs when the lift distribution on a wing is elliptic. For an untwisted wing this corresponds to an elliptic chord distribution.

12.11 Induced drag of a rectangular wing

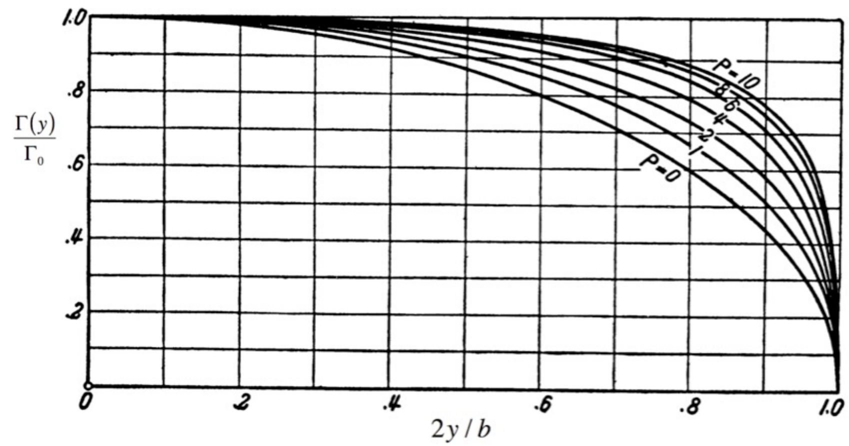

Figure 12.27 Circulation distribution along straight wings of various aspect ratios from Prandtl & Tietjens (Applied Hydro and Aeromechanics). The aspect ratio parameter is $P = (2/\pi)b/C$.

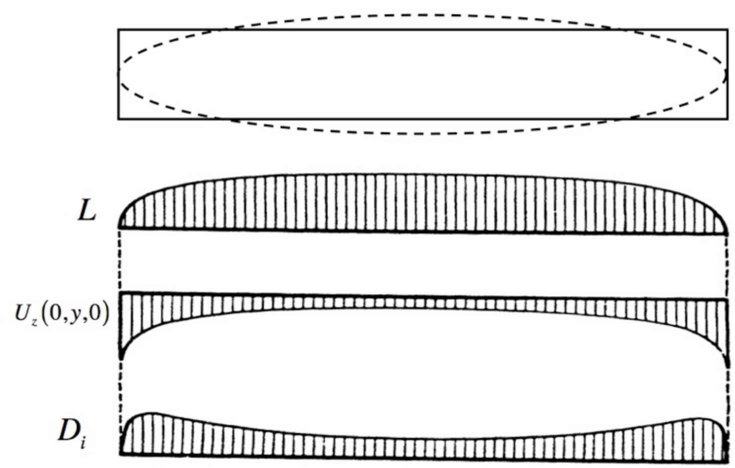

Figure 12.28 Typical variations of lift, downwash and induced drag for a rectangular wing from Prandtl & Tietjens.

$$\frac{D_i}{D_{i\,\min}} = 0.99 + 0.015\left(\frac{2b}{\pi C}\right) \qquad (12.179)$$

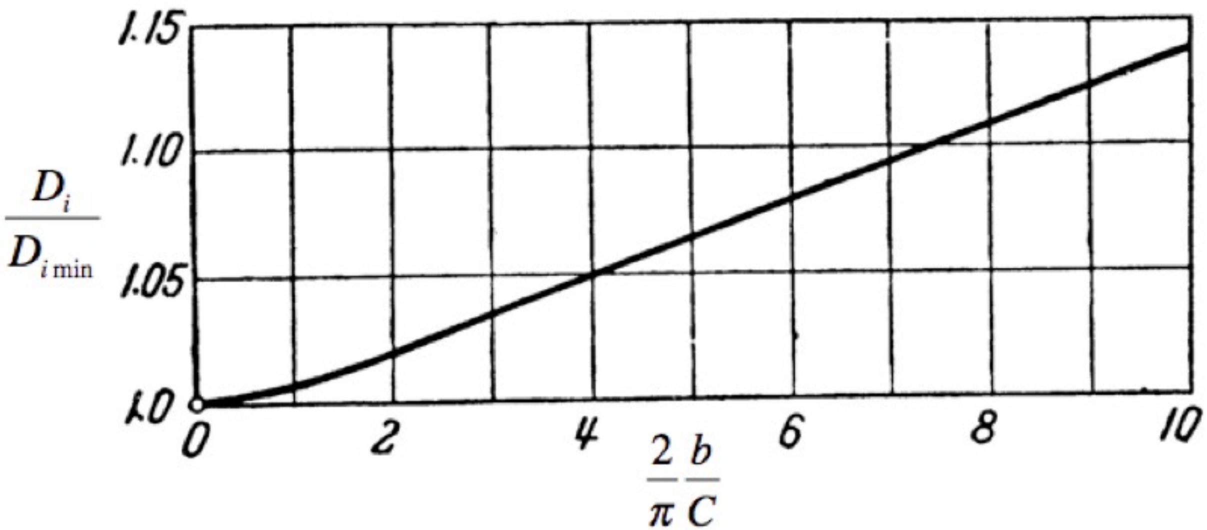

Figure 12.29 Induced drag of a straight wing of varying aspect ratio compared to the induced drag of an elliptic wing $D_{i\,\min}$ from Prandtl & Tietjens.

Recall the induced drag result for an elliptic wing

$$C_{Di} = \frac{C_L^2}{\pi}\frac{S}{b^2} \qquad (12.180)$$

Profile drag is the sum of viscous drag plus pressure drag due to the deviation of the pressure field from the potential flow solution.

$$C_D = C_{Di} + C_{Dp} \qquad (12.182)$$

On a real wing profile drag is almost independent of angle of attack.

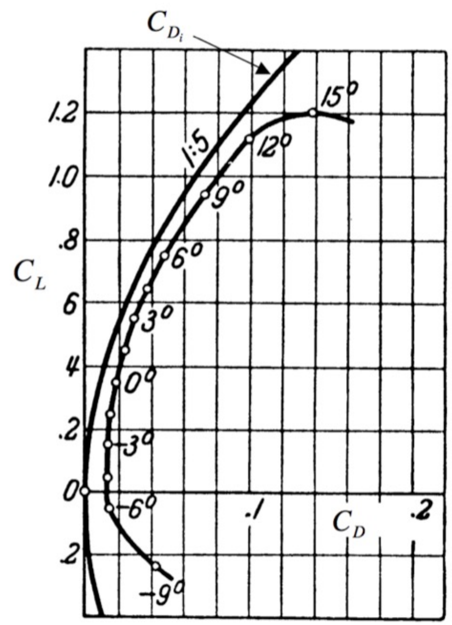

From Prandtl and Tietjens

Figure 12.30 Lift-drag parabola for a rectangular wing with aspect ratio parameter $P = (2/\pi)b/C = 5$ compared to the induced drag of a rectangular wing.

Consider two wings with the same profile but different aspect ratio

$$C_{D_1} = \frac{C_L^2}{\pi}\frac{S_1}{b_1^2} + C_{Dp}$$
$$C_{D_2} = \frac{C_L^2}{\pi}\frac{S_2}{b_2^2} + C_{Dp} \qquad (12.183)$$

Since the profile drag coefficient is the same for both wings the drag coefficient of one wing can be converted to the other using

$$C_{D_2} = C_{D_1} + \frac{C_L^2}{\pi}\left(\frac{S_2}{b_2^2} - \frac{S_1}{b_1^2}\right) \qquad (12.184)$$

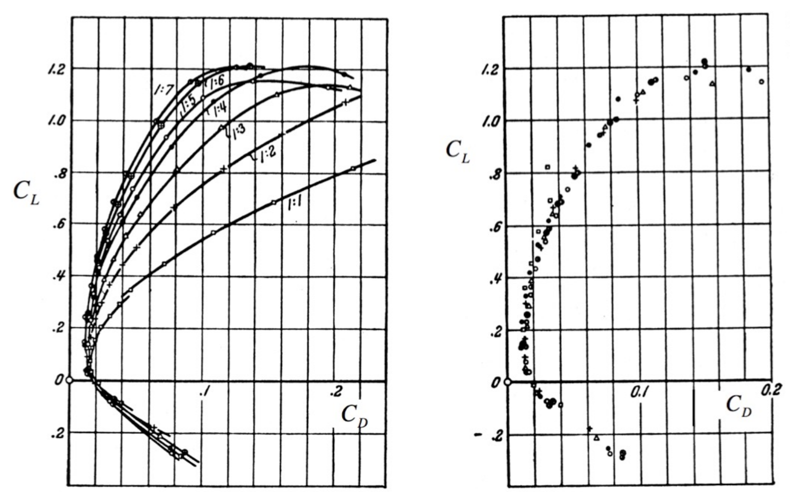

Figure 12.31 Left, lift-drag parabola for a rectangular wing of various aspect ratios. Same data scaled to $P = (2/\pi)b/C = 5$ using (12.184).

From Prandtl and Tietjens

The same idea can be used to collapse lift data. Recall the downwash velocity for an elliptic wing

$$U_z(0,y,0) = -\frac{\Gamma_0}{2b} \tag{12.185}$$

Recall the lift for an elliptic wing

$$L = \left(\frac{\pi}{4}\right)\rho U_\infty \Gamma_0 b \tag{12.186}$$

$$C_L = \frac{L}{\frac{1}{2}\rho U_\infty^2 S} = \left(\frac{\pi}{2}\right)\frac{\Gamma_0}{U_\infty S} \tag{12.187}$$

Combine 12.185 and 12.187

$$\frac{U_z}{U_\infty} = -\frac{\Gamma_0}{2bU_\infty} = -\frac{C_L}{\pi}\frac{S}{b^2} \tag{12.188}$$

Recall that one of the effects of the downwash of a finite wing is to decrease the effective angle of attack of the wing and thereby reduce the lift. If a section of a finite wing were to have the same lift as the same section considered to be part of an infinite wing at angle of attack α_0 its angle of attack would have to be increased by $-\alpha_i = \frac{C_L}{\pi}\frac{S}{b^2}$. The angle of attack of the wing would need to be

$$\alpha = \alpha_0 - \alpha_i = \alpha_0 + \frac{C_L}{\pi}\frac{S}{b^2} \tag{12.189}$$

Consider two wings with the same profile but different aspect ratio

$$\alpha_1 = \alpha_0 + \frac{C_L}{\pi}\frac{S_1}{b_1^2}$$
$$\alpha_2 = \alpha_0 + \frac{C_L}{\pi}\frac{S_2}{b_2^2} \qquad (12.190)$$

Since the reference angle of attack is the same for both wings the angle of attack of one wing can be converted to the other using

$$\alpha_2 = \alpha_1 + \frac{C_L}{\pi}\left(\frac{S_2}{b_2^2} - \frac{S_1}{b_1^2}\right) \qquad (12.191)$$

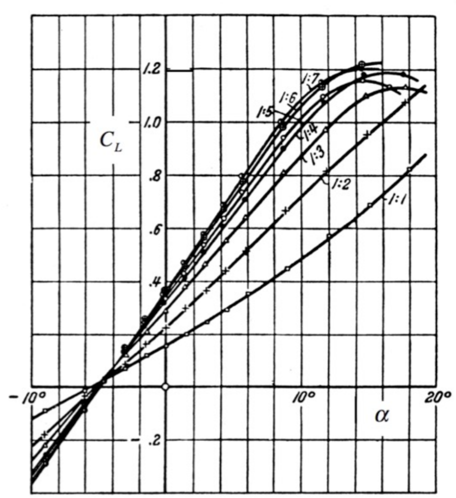

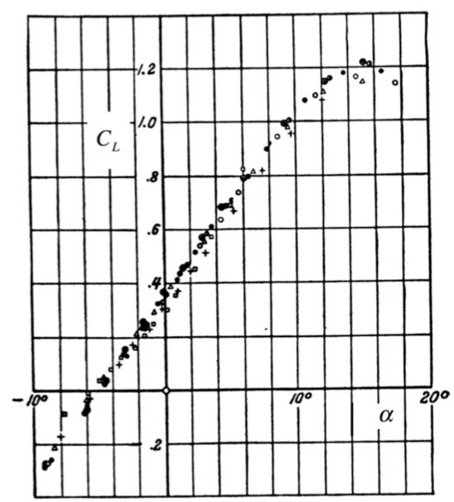

From Prandtl and Tietjens

Figure 12.32 Left, Lift versus angle-of-attack for a rectangular wing of various aspect ratios. Same data scaled to $P = (2/\pi)b/C = 5$ *using* (12.191).

12.12 Unsteady momentum integral in a Trefftz plane fixed with respect to the surrounding fluid

A 3-D momentum balance on a point force (see Chapter 10 section 10) suggests that two-thirds of the applied impulse by a lifting aircraft in steady flight is contained in the downward momentum generated by the force

$$U_\infty t \int_{-\infty}^{\infty}\int_{-\infty}^{\infty} U_z \, dy\, dz = -\frac{2}{3}\frac{L}{\rho}u(t)t \qquad (12.192)$$

$$\int_{-\infty}^{\infty}\int_{-\infty}^{\infty} U_z \, dy\, dz = -\frac{2}{3}\left(\frac{L}{\rho U_\infty}\right) \qquad (12.193)$$

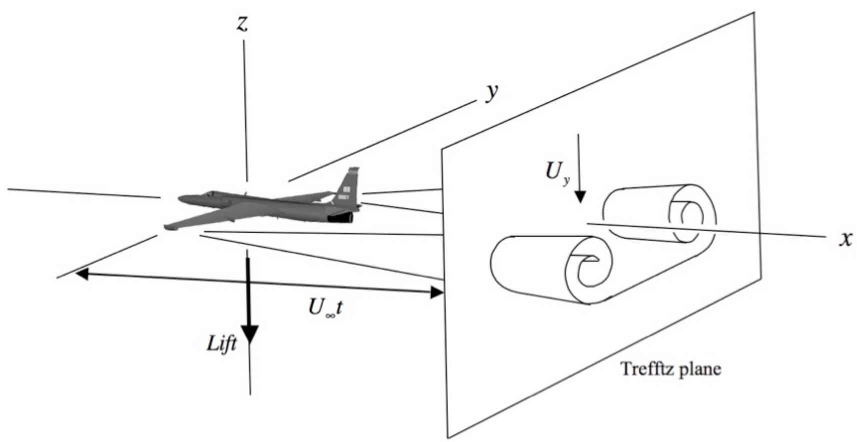

Figure 12.33 Aircraft wake with Trefftz plane fixed with respect to the surrounding fluid

Carry out a 2-D momentum balance on an infinite impulsive line force

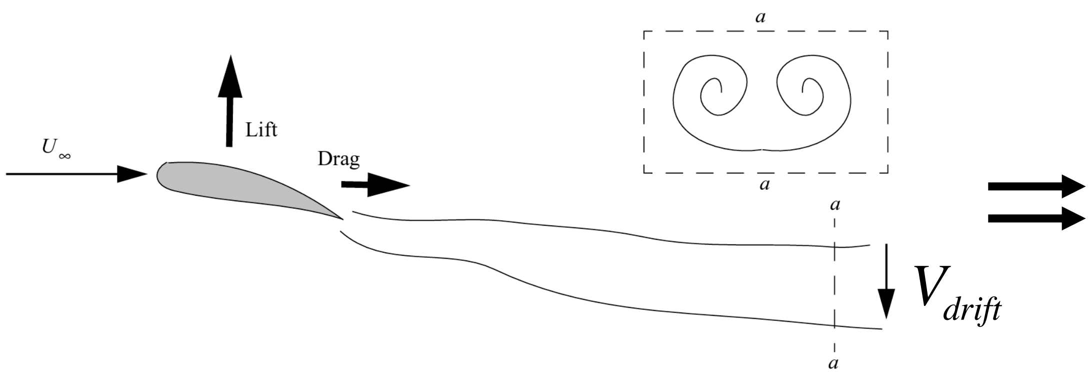

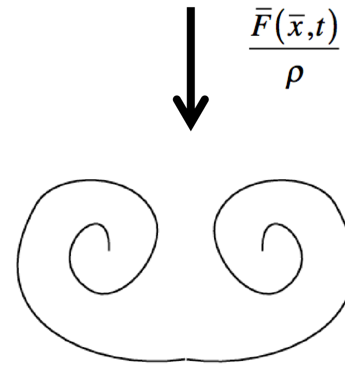

$$\frac{\bar{F}(\bar{x},t)}{\rho} = \left\{0, -\frac{I}{\rho}\delta(t)\delta(y)\delta(z)\right\}$$

$$\frac{I}{\rho} = \frac{L}{\rho U_\infty}$$

Impulse per unit length of aircraft wake

$$\frac{D}{Dt}\left(\int_A \bar{U}\,dA\right) + \int_C \left(\bar{U}\bar{U} + \frac{P}{\rho}\bar{\bar{I}}\right)\bullet \hat{n}\,dC + \nu\int_C \left(\hat{n}\times\bar{\Omega}\right)dA = \int_A \left(\frac{F(\bar{x},t)}{\rho}\right)dA \qquad (12.194)$$

where C is a fixed circular contour of large radius R surrounding the 2-D momentum source (force) located at the origin. The force divided by density acting on the flow is really a force per unit length with units L^3/T instead of L^4/T as in the 3-D case. In the far field the velocity behaves as $\bar{U} \sim 1/R^2$, the vorticity is zero and the momentum balance becomes

$$\lim_{R\to\infty}\frac{D}{Dt}\left(\int_A \bar{U}\,dA\right) + \int_C \left(\frac{P}{\rho}\bar{\bar{I}}\right)\bullet \hat{n}\,dC = \int_A \left(\frac{F(\bar{x},t)}{\rho}\right)dA \qquad (12.195)$$

STANFORD AERONAUTICS & ASTRONAUTICS

The impulsive force creating the flow is

$$\frac{\bar{F}(\bar{x},t)}{\rho} = \left\{0, -\frac{I}{\rho}\delta(t)\delta(y)\delta(z)\right\} \qquad (12.196)$$

Total impulse produced by a force

$$\frac{\bar{I}}{\rho} = \left\{0, \int_0^t \frac{I}{\rho}\delta(t)\,dt\right\} = \left\{0, \frac{I}{\rho}\right\} \qquad (12.197)$$

Momentum balance

$$\lim_{R\to\infty} \frac{D}{Dt}\left(\int_A U_z\, dA\right) + \lim_{R\to\infty} \int_C \left(\frac{P}{\rho}\bar{\bar{I}}\right) \bullet \hat{n}\, dC \Bigg|_z = -\frac{I}{\rho}\delta(t) \qquad (12.198)$$

Far field vector potential

$$\bar{A} = \{A_x, A_y, A_z\} = \left\{-\frac{I}{2\pi\rho}u(t)\frac{y}{(y^2+z^2)}, 0, 0\right\} \tag{12.199}$$

Far field velocity

$$\bar{U} = \{U_y, U_z\} = \left\{\frac{I}{\pi\rho}u(t)\frac{yz}{(y^2+z^2)^2}, \frac{I}{2\pi\rho}u(t)\left(-\frac{2y^2}{(y^2+z^2)^2}+\frac{1}{(y^2+z^2)}\right)\right\} \tag{12.200}$$

Far field scalar potential

Far field flow is a dipole

$$\Phi = \frac{I}{2\pi\rho}u(t)\left(\frac{z}{y^2+z^2}\right) \tag{12.201}$$

Far field pressure disturbance

$$\frac{\partial \bar{U}}{\partial t} + \nabla\left(\frac{P}{\rho}\right) = 0 \Rightarrow \frac{P}{\rho} = -\frac{\partial \phi}{\partial t} \tag{12.202}$$

$$\frac{P}{\rho} = -\frac{I}{2\pi\rho}\delta(t)\left(\frac{z}{y^2+z^2}\right) \tag{12.203}$$

STANFORD
AERONAUTICS & ASTRONAUTICS

Integrate the pressure

$$\lim_{R\to\infty}\int_C\left(\frac{P}{\rho}\overline{\overline{I}}\right)\bullet\hat{n}\,dC\Bigg|_z=-\frac{I}{2\pi\rho}\delta(t)\int_0^{2\pi}Sin^2(\theta)\,d\theta=-\frac{1}{2}\frac{I}{\rho}\delta(t) \qquad (12.204)$$

Rate of change of the total downward momentum

$$\lim_{R\to\infty}\frac{D}{Dt}\left(\int_A U_z\,dA\right)=-\frac{1}{2}\frac{I}{\rho}\delta(t) \qquad (12.205)$$

Momentum integral is one-half the applied impulse

$$H_z=\int_{-\infty}^{\infty}\int_{-\infty}^{\infty}U_z\,dydz=-\frac{1}{2}\frac{I}{\rho} \qquad (12.206)$$

Impulse is related to the lift

$$\frac{I}{\rho}=\frac{L}{\rho U_\infty} \qquad (12.207)$$

Momentum integral related to lift

$$H_z=\int_{-\infty}^{\infty}\int_{-\infty}^{\infty}U_z\,dydz=-\frac{1}{2}\frac{L}{\rho U_\infty} \qquad (12.208)$$

12.13 Inviscid vortex pair model of the wake

We need to determine b_0 and a(t)

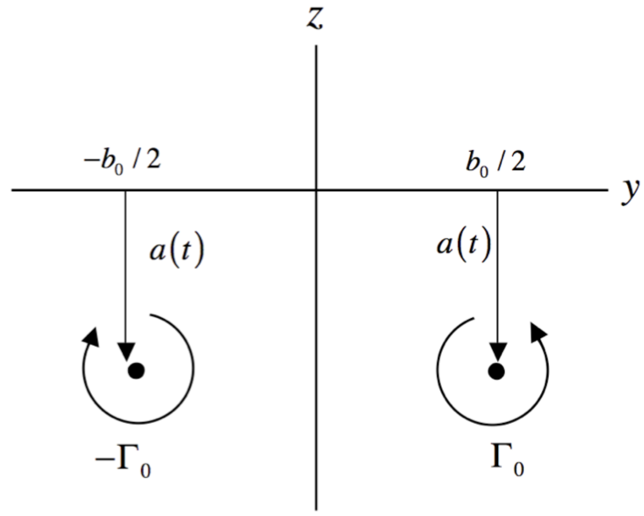

Figure 12.34 Inviscid vortex pair.

$$a(t) > 0$$

Vortex position
z = - a(t)

Vorticity source - one vortex

$$\bar{\Omega}(\bar{x},t) = \left\{\Gamma_0\delta(y-b_0/2)\delta(z+a(t)),0,0\right\} \tag{12.209}$$

3D vector potential - one vortex

$$\begin{aligned}
A_x &= \frac{1}{4\pi}\int_{-\infty}^{\infty}\int_{-\infty}^{\infty}\int_{-\infty}^{\infty}\frac{\Gamma_0\delta(y_s-b_0/2)\delta(z_s+a(t))}{\left((x-x_s)^2+(y-y_s)^2+(z-z_s)^2\right)^{1/2}}dx_s\,dy_s\,dz_s = \\
A_x &= \frac{\Gamma_0}{4\pi}\int_{-\infty}^{\infty}\frac{1}{\left((x-x_s)^2+(y-b_0/2)^2+(z+a(t))^2\right)^{1/2}}dx_s
\end{aligned} \tag{12.210}$$

3D vector potential - two vortices

$$A_x = \frac{\Gamma_0}{4\pi}\lim_{\lambda\to\infty} Ln\left(\frac{\lambda + x + \sqrt{(x+\lambda)^2 + (y-b_0/2)^2 + (z+a(t))^2}}{-\lambda + x + \sqrt{(x-\lambda)^2 + (y-b_0/2)^2 + (z+a(t))^2}}\right) \tag{12.211}$$

2D vector potential of one vortex

$$A_x = -\frac{\Gamma_0}{2\pi}\left(Ln\left((y-b_0/2)^2 + (z+a(t))^2\right)^{1/2} - Ln(2)\right)$$
$$A_x = -\frac{\Gamma_0}{2\pi}Ln\left(\frac{\left((y-b_0/2)^2 + (z+a(t))^2\right)^{1/2}}{2}\right) \tag{12.212}$$

2D vector potential of two vortices

$$A_x = -\frac{\Gamma_0}{4\pi}Ln\left(\frac{(y-b_0/2)^2 + (z+a(t))^2}{(y+b_0/2)^2 + (z+a(t))^2}\right) \tag{12.213}$$

2D scalar potential of two vortices

$$\Phi(y,z) = \frac{\Gamma_0}{2\pi}\left(ArcTan\left(\frac{z+a(t)}{y-b_0/2}\right) - ArcTan\left(\frac{z+a(t)}{y+b_0/2}\right)\right) \tag{12.214}$$

STANFORD AERONAUTICS & ASTRONAUTICS

Velocity field of an inviscid vortex pair

$$\bar{U} = \{U_y, U_z\} = \left(\frac{\Gamma_0 b_0}{2\pi\left((y-b_0/2)^2+(z+a(t))^2\right)\left((y+b_0/2)^2+(z+a(t))^2\right)}\right)\times$$

$$\left(-2y(z+a(t)),\left(y^2-\left(\frac{b_0}{2}\right)^2-(z+a(t))^2\right)\right) \qquad (12.215)$$

$$U_y = \frac{\Gamma_0}{2\pi}\left(\frac{-(z+a)}{(z+a)^2+(y-b_0/2)^2}+\frac{(z+a)}{(z+a)^2+(y+b_0/2)^2}\right)$$

$$U_z = \frac{\Gamma_0}{2\pi}\left(\frac{(y-b_0/2)}{(z+a)^2+(y-b_0/2)^2}-\frac{(y+b_0/2)}{(z+a)^2+(y+b_0/2)^2}\right)$$

STANFORD AERONAUTICS & ASTRONAUTICS

Momentum of an inviscid vortex pair

$$\bar{H} = \int_{-\infty}^{\infty}\int_{-\infty}^{\infty} \bar{U}\, dz\, dy = \int_{0}^{2\pi} \Phi r \hat{n} d\theta$$

$$\frac{\Gamma_0}{2\pi}\int_0^{2\pi}\left(ArcTan\left(\frac{rSin(\theta)+a(t)}{rCos(\theta)-b_0/2}\right)-ArcTan\left(\frac{rSin(\theta)+a(t)}{rCos(\theta)+b_0/2}\right)\right)r\{Cos(\theta),Sin(\theta)\}d\theta \tag{12.216}$$

$$ArcTan(u)-ArcTan(v)=ArcTan\left(\frac{u-v}{1-uv}\right) \tag{12.217}$$

$$\frac{u-v}{1-uv}=\frac{b_0\left(rSin(\theta)+a(t)\right)}{r^2Cos^2(\theta)-(b_0/2)^2-\left(rSin(\theta)+a(t)\right)^2} \tag{12.218}$$

$$\bar{H} = \int_{-\infty}^{\infty}\int_{-\infty}^{\infty} \bar{U}\, dz\, dy =$$

$$\frac{\Gamma_0}{2\pi}\int_0^{2\pi}\left(ArcTan\left(\frac{b_0\left(rSin(\theta)+a(t)\right)}{r^2Cos^2(\theta)-(b_0/2)^2-\left(rSin(\theta)+a(t)\right)^2}\right)\right)r\{Cos(\theta),Sin(\theta)\}d\theta \tag{12.219}$$

Momentum integral of an inviscid vortex pair

$$\bar{H}=\{H_y,H_z\}=\left\{0,-\frac{\Gamma_0 b_0}{2}\right\} \tag{12.220}$$

STANFORD AERONAUTICS & ASTRONAUTICS

Recall the connection to aircraft lift 12.208

$$H_z = \int_{-\infty}^{\infty}\int_{-\infty}^{\infty} U_z \, dy\, dz = -\frac{1}{2}\frac{L}{\rho U_\infty}$$

$$H_z = -\frac{\Gamma_0 b_0}{2}$$

$$L = \rho U_\infty \Gamma_0 b_0 \qquad (12.221)$$

For an elliptic wing

$$L = \rho U_\infty \Gamma_0 \left(\frac{\pi}{4} b\right) \qquad (12.222)$$

Vortex spacing needed to match the lift of an elliptic wing

$$b_0 = \frac{\pi}{4} b \qquad (12.223)$$

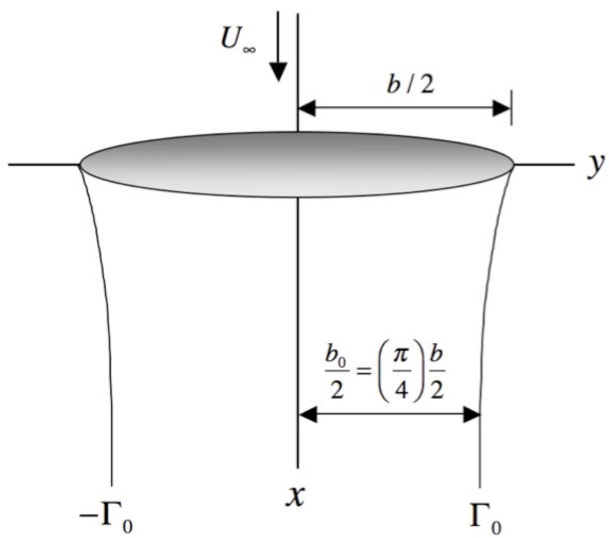

Figure 12.35 Vortex spacing in the wake of an elliptically loaded wing.

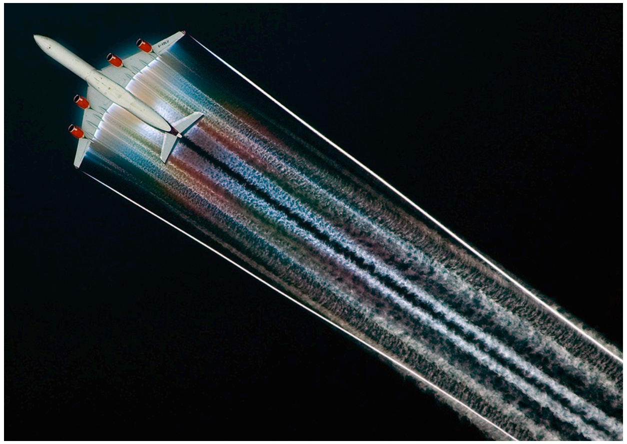

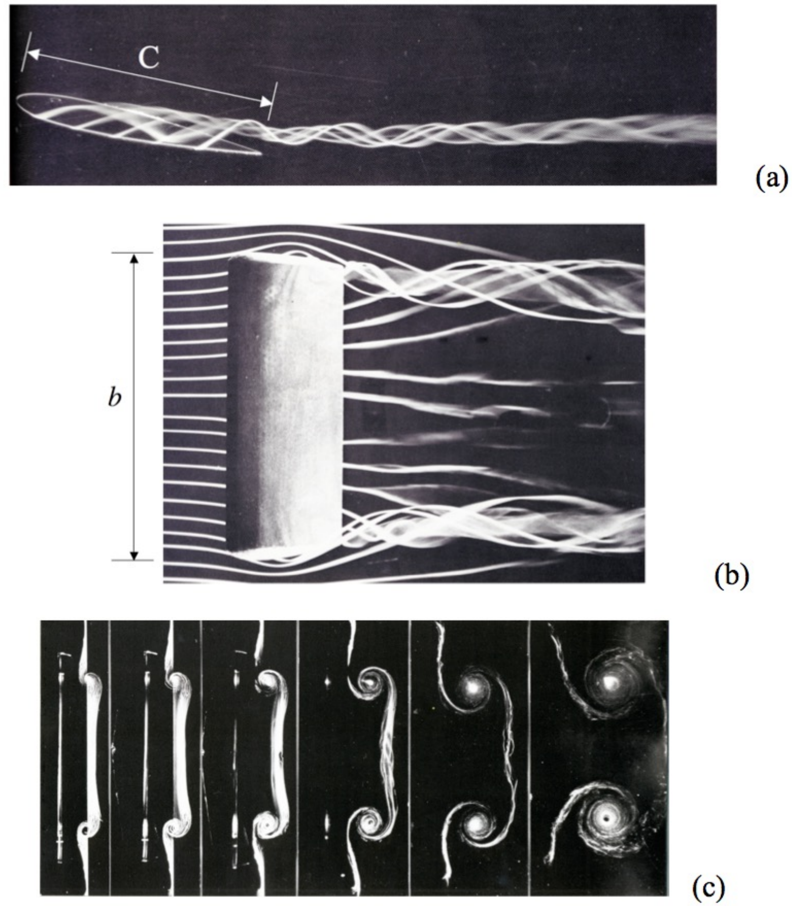

Figure 12.1 Images of the flow past a finite span wing at low speed. From An Album of Fluid Motion by M. Van Dyke.

What about a(t) - require no net pressure on the vortex pair

z-momentum on the z-axis

$$-\frac{\partial}{\partial z}\left(\frac{P(0,z)}{\rho}\right)=\frac{\partial U_z(0,z)}{\partial t}+U_z(0,z)\frac{\partial U_z(0,z)}{\partial z}=$$
$$\frac{\partial U_z(0,z)}{\partial a}\frac{da}{dt}+U_z(0,z)\frac{\partial U_z(0,z)}{\partial z}=\frac{\partial U_z(0,z)}{\partial z}\frac{da}{dt}+U_z(0,z)\frac{\partial U_z(0,z)}{\partial z} \quad (12.225)$$

Pressure on the z-axis

$$-\left(\frac{P}{\rho}-\frac{P_\infty}{\rho}\right)=\left(U_z(0,z)\frac{da}{dt}+\frac{1}{2}U_z(0,z)^2\right)$$

Net pressure integrated along the z-axis should be zero

$$-\int_{-\infty}^{\infty}\left(\frac{P}{\rho}-\frac{P_\infty}{\rho}\right)dz=\int_{-\infty}^{\infty}\left(U_z(0,z)\frac{da}{dt}+\frac{1}{2}U_z(0,z)^2\right)dz=0 \quad (12.226)$$

$$\frac{da}{dt}=-\frac{1}{2}\frac{\int_{-\infty}^{\infty}\left(U_z(0,z)^2\right)dz}{\int_{-\infty}^{\infty}\left(U_z(0,z)\right)dz} \quad (12.227)$$

z-velocity on the z-axis

$$U_z(0,z) = -\frac{\Gamma_0 b_0}{2\pi}\left(\frac{1}{(z+a)^2+\left(\frac{b_0}{2}\right)^2}\right) \qquad (12.228)$$

$$\frac{da}{dt} = \frac{\Gamma_0 b_0}{4\pi}\frac{\int_{-\infty}^{\infty}\left(1/\left((z+a)^2+\left(\frac{b_0}{2}\right)^2\right)\right)^2 dz}{\int_{-\infty}^{\infty}\left(1/\left((z+a)^2+\left(\frac{b_0}{2}\right)^2\right)\right)dz} =$$

$$\frac{da}{dt} = \frac{\Gamma_0 b_0}{4\pi}\frac{1}{\left(\frac{b_0}{2}\right)^2}\frac{\int_{-\infty}^{\infty}\left(1/\left(\left(\frac{z+a}{b_0/2}\right)^2+1\right)\right)^2 d\left(\frac{z+a}{b_0/2}\right)}{\int_{-\infty}^{\infty}\left(1/\left(\left(\frac{z+a}{b_0/2}\right)^2+1\right)\right)d\left(\frac{z+a}{b_0/2}\right)} = \frac{\Gamma_0}{2\pi b_0} \qquad (12.229)$$

Downward drift speed of the vortex pair

STANFORD AERONAUTICS & ASTRONAUTICS

Recall unsteady scalar potential, vector potential and velocity

$$\Phi(y,z)=\frac{\Gamma_0}{2\pi}\left(ArcTan\left(\frac{z+\dfrac{\Gamma_0 t}{2\pi b_0}}{y-b_0/2}\right)-ArcTan\left(\frac{z+\dfrac{\Gamma_0 t}{2\pi b_0}}{y+b_0/2}\right)\right) \qquad (12.230)$$

$$A_x=-\frac{\Gamma_0}{4\pi}Ln\left(\frac{\left(y-b_0/2\right)^2+\left(z+\dfrac{\Gamma_0 t}{2\pi b_0}\right)^2}{\left(y+b_0/2\right)^2+\left(z+\dfrac{\Gamma_0 t}{2\pi b_0}\right)^2}\right) \qquad (12.231)$$

$$\begin{aligned}
U_y&=\frac{\Gamma_0}{2\pi}\left(\frac{-\left(z+\dfrac{\Gamma_0 t}{2\pi b_0}\right)}{\left(z+\dfrac{\Gamma_0 t}{2\pi b_0}\right)^2+\left(y-\dfrac{b_0}{2}\right)^2}+\frac{\left(z+\dfrac{\Gamma_0 t}{2\pi b_0}\right)}{\left(z+\dfrac{\Gamma_0 t}{2\pi b_0}\right)^2+\left(y+\dfrac{b_0}{2}\right)^2}\right)\\
U_z&=\frac{\Gamma_0}{2\pi}\left(\frac{\left(y-\dfrac{b_0}{2}\right)}{\left(z+\dfrac{\Gamma_0 t}{2\pi b_0}\right)^2+\left(y-\dfrac{b_0}{2}\right)^2}-\frac{\left(y+\dfrac{b_0}{2}\right)}{\left(z+\dfrac{\Gamma_0 t}{2\pi b_0}\right)^2+\left(y+\dfrac{b_0}{2}\right)^2}\right)
\end{aligned} \qquad (12.232)$$

Transform to an observer moving downward with the vortex pair

$$
\begin{aligned}
\tilde{y} &= y \\
\tilde{z} &= z + \frac{\Gamma_0 t}{2\pi b_0} \\
\tilde{U}_{\tilde{y}} &= U_y \\
\tilde{U}_{\tilde{z}} &= U_z + \frac{\Gamma_0}{2\pi b_0} \\
\tilde{P} &= P \\
\tilde{A}_{\tilde{x}} &= A_x - \frac{\Gamma_0 y}{2\pi b_0} \\
\tilde{\Phi} &= \Phi + \frac{\Gamma_0}{2\pi b_0}\left(z + \frac{\Gamma_0 t}{2\pi b_0}\right)
\end{aligned}
\qquad (12.233)
$$

$$
\tilde{\Phi}(\tilde{y},\tilde{z}) = \frac{\Gamma_0}{2\pi}\left(ArcTan\left(\frac{\tilde{z}}{\tilde{y} - b_0/2}\right) - ArcTan\left(\frac{\tilde{z}}{\tilde{y} + b_0/2}\right)\right) + \frac{\Gamma_0 \tilde{z}}{2\pi b_0} \qquad (12.234)
$$

$$
\tilde{A}_{\tilde{x}}(\tilde{y},\tilde{z}) = -\frac{\Gamma_0}{4\pi} Ln\left(\frac{(\tilde{y} - b_0/2)^2 + \tilde{z}^2}{(\tilde{y} + b_0/2)^2 + \tilde{z}^2}\right) - \frac{\Gamma_0 \tilde{y}}{2\pi b_0} \qquad (12.235)
$$

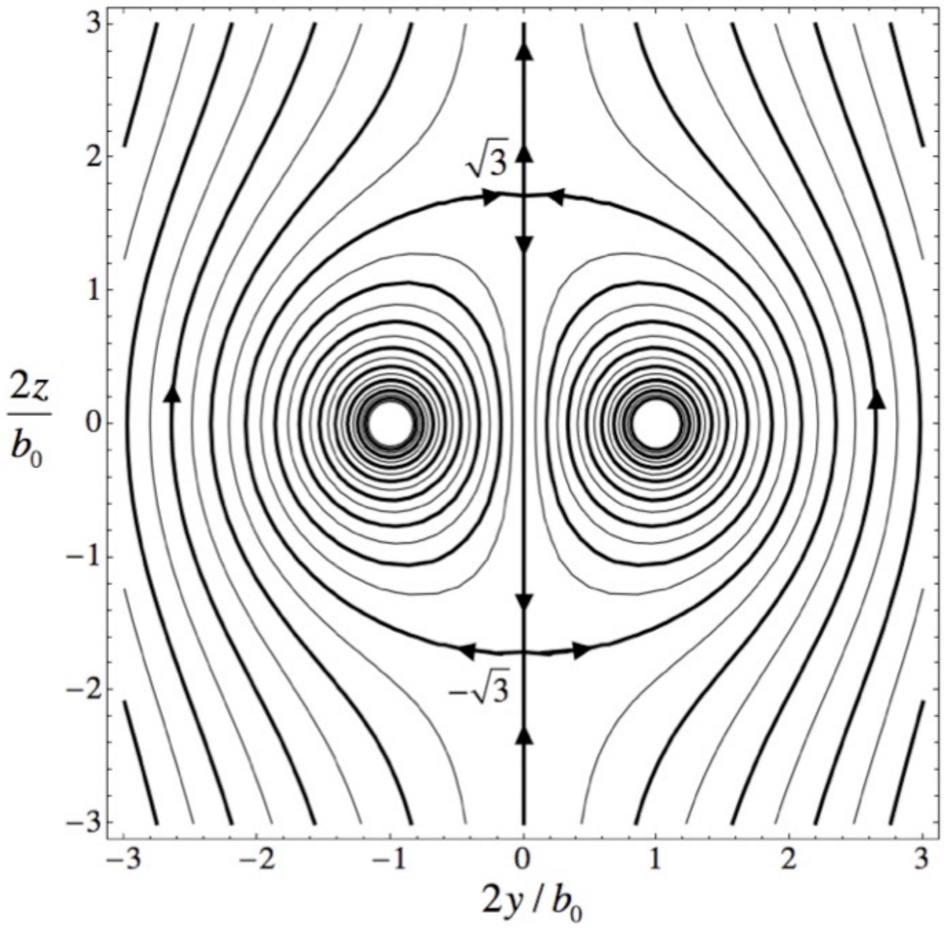

Figure 12.36 Streamline pattern of an inviscid trailing vortex pair as seen by an observer convecting downward with the pair.

A plausible correction to the induced drag

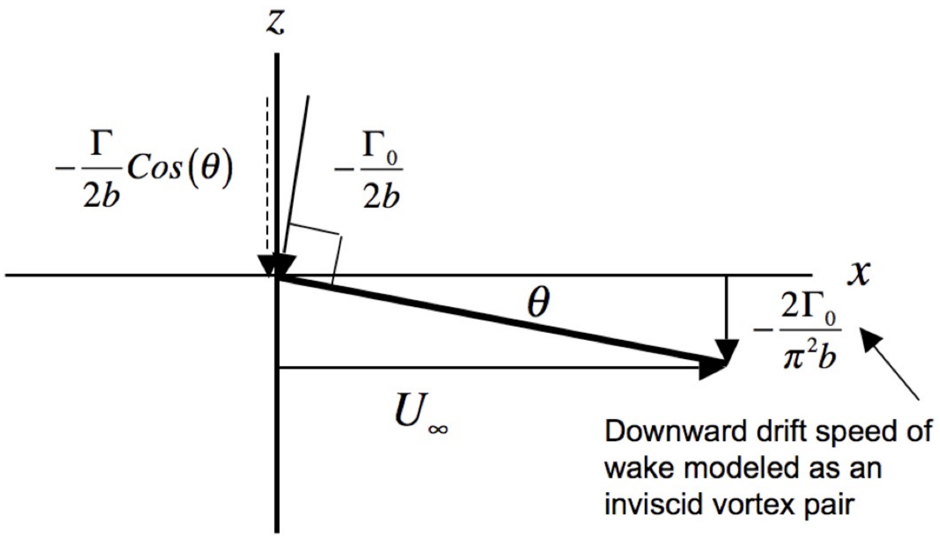

Downward drift speed of the vortex pair created by an elliptic wing based on wing span

$$U_{ydrift} = -2\Gamma_0 / \left(\pi^2 b\right)$$

$$U_z(0,y,0) = -\frac{\Gamma}{2b}Cos(\theta)$$

$$\frac{U_z(0,y,0)}{U_\infty} \doteq -\frac{\Gamma_0}{2bU_\infty}\left(1 - \frac{16}{2\pi^4}\left(\frac{\Gamma}{2bU_\infty}\right)^2\right)$$

Oswald efficiency

$$C_{Di} = \frac{C_L^2}{\pi}\frac{S}{b^2} \qquad (12.180)$$

Recall for an elliptic wing

$$C_D = C_{Di} + C_{Dp} \qquad (12.182)$$

The Oswald efficiency is used to adjust for a non-elliptic lift distribution

Typically between 0.7 and 0.9

$$C_D = C_{Dp} + \frac{C_L^2}{\varepsilon_0 \pi}\frac{S}{b^2}$$

Span efficiency

in practice the profile drag may have a small quadratic dependence on the square of the lift coefficient.

$$C_D = C_{Dp0} + C_{Dp1} {C_L}^2 + \frac{{C_L}^2}{\varepsilon_1 \pi}\frac{S}{b^2}$$

12.14 Effect of a ground plane on the downwash velocity

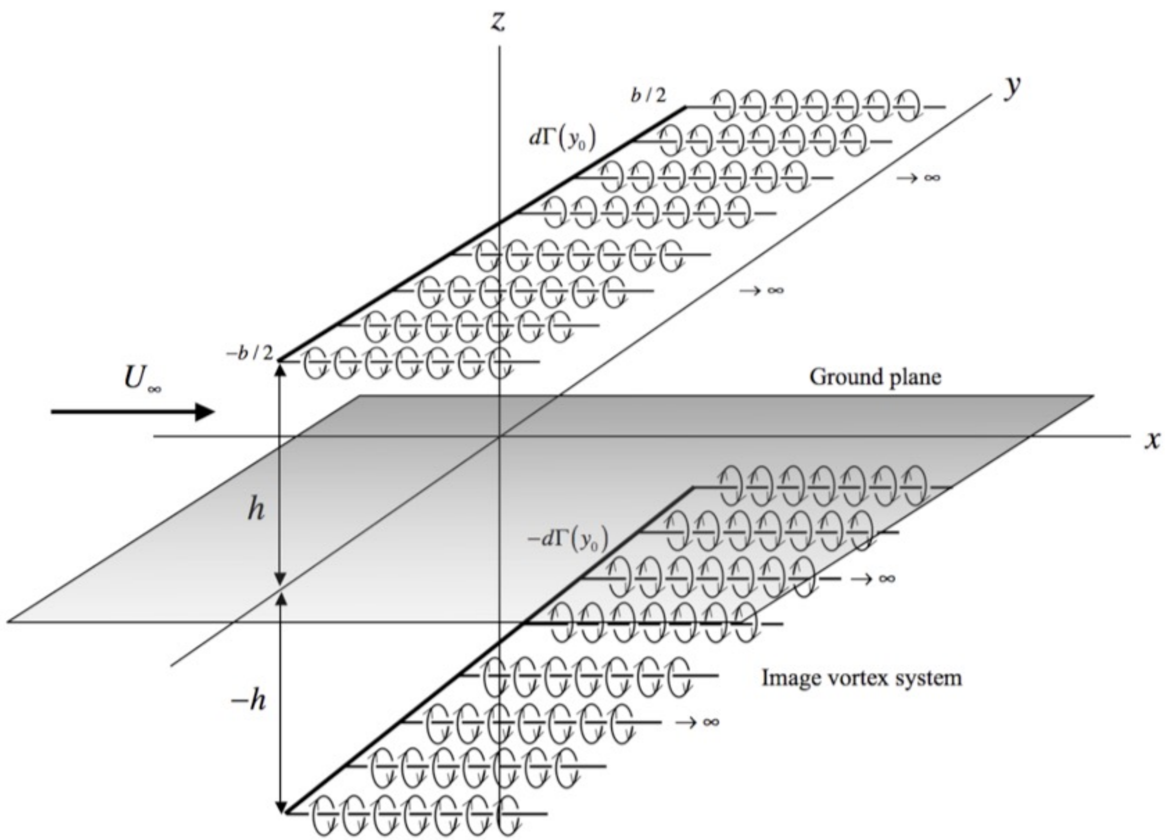

Figure 12.37 Continuous distribution of vortex lines with image system beneath the ground plane.

STANFORD
AERONAUTICS & ASTRONAUTICS

Vector potential of the main vortex sheet plus the image sheet below the ground plane

$$A_x(x,y,z) = -\frac{1}{4\pi}\int_0^{b/2}\left(\frac{d\Gamma(y_0)}{dy_0}\right)\times$$

$$\left(Ln\left(\frac{x+\left(x^2+(y+y_0)^2+(z-h)^2\right)^{1/2}\left((y-y_0)^2+(z-h)^2\right)}{\left(x+\left(x^2+(y-y_0)^2+(z-h)^2\right)^{1/2}\right)\left((y+y_0)^2+(z-h)^2\right)}\right) - Ln\left(\frac{x+\left(x^2+(y+y_0)^2+(z+h)^2\right)^{1/2}\left((y-y_0)^2+(z+h)^2\right)}{\left(x+\left(x^2+(y-y_0)^2+(z+h)^2\right)^{1/2}\right)\left((y+y_0)^2+(z+h)^2\right)}\right)\right) dy_0 \qquad (12.237)$$

Velocity field

$$U_z(x,y,z) = \frac{\Gamma_0}{2\pi b}\int_0^{b/2} \frac{\left(\frac{2y_0}{b}\right)}{\left(1-\left(\frac{2y_0}{b}\right)^2\right)^{1/2}} \times$$

$$\left(\frac{-(y-y_0)\left((y+y_0)^2+(z-h)^2\right)-2(y+y_0)\left(x+\left(x^2+(y-y_0)^2+(z-h)^2\right)^{1/2}\right)\left(x^2+(y-y_0)^2+(z-h)^2\right)^{1/2}}{\left(x^2+(y-y_0)^2+(z-h)^2\right)^{1/2}\left(x+\left(x^2+(y-y_0)^2+(z-h)^2\right)^{1/2}\right)\left((y+y_0)^2+(z-h)^2\right)} + \frac{(y+y_0)\left((y-y_0)^2+(z-h)^2\right)+2(y-y_0)\left(x+\left(x^2+(y+y_0)^2+(z-h)^2\right)^{1/2}\right)\left(x^2+(y+y_0)^2+(z-h)^2\right)^{1/2}}{\left(x^2+(y+y_0)^2+(z-h)^2\right)^{1/2}\left(x+\left(x^2+(y+y_0)^2+(z-h)^2\right)^{1/2}\right)\left((y-y_0)^2+(z-h)^2\right)} \right) dy_0 -$$

$$\frac{\Gamma_0}{2\pi b}\int_0^{b/2} \frac{\left(\frac{2y_0}{b}\right)}{\left(1-\left(\frac{2y_0}{b}\right)^2\right)^{1/2}} \times$$

$$\left(\frac{-(y-y_0)\left((y+y_0)^2+(z+h)^2\right)-2(y+y_0)\left(x+\left(x^2+(y-y_0)^2+(z+h)^2\right)^{1/2}\right)\left(x^2+(y-y_0)^2+(z+h)^2\right)^{1/2}}{\left(x^2+(y-y_0)^2+(z+h)^2\right)^{1/2}\left(x+\left(x^2+(y-y_0)^2+(z+h)^2\right)^{1/2}\right)\left((y+y_0)^2+(z+h)^2\right)} + \frac{(y+y_0)\left((y-y_0)^2+(z+h)^2\right)+2(y-y_0)\left(x+\left(x^2+(y+y_0)^2+(z+h)^2\right)^{1/2}\right)\left(x^2+(y+y_0)^2+(z+h)^2\right)^{1/2}}{\left(x^2+(y+y_0)^2+(z+h)^2\right)^{1/2}\left(x+\left(x^2+(y+y_0)^2+(z+h)^2\right)^{1/2}\right)\left((y-y_0)^2+(z+h)^2\right)} \right) dy_0$$

(12.238)

STANFORD
AERONAUTICS & ASTRONAUTICS

On the lifting line

$$U_z(0,0,h) = -\frac{\Gamma_0}{\pi b}\left(\int_0^1 \frac{1}{\left(1-\left(\frac{2y_0}{b}\right)^2\right)^{1/2}} d\left(\frac{2y_0}{b}\right) - \int_0^1 \frac{\left(\frac{2y_0}{b}\right)^2}{\left(1-\left(\frac{2y_0}{b}\right)^2\right)^{1/2}\left(\left(\frac{2y_0}{b}\right)^2+4\left(\frac{2h}{b}\right)^2\right)} d\left(\frac{2y_0}{b}\right) \right) \quad (12.239)$$

Which integrates to

$$U_z(0,0,h) = -\frac{\Gamma_0}{2b}\left(\frac{\left(4\frac{h}{b}\right)}{\sqrt{1+\left(4\frac{h}{b}\right)^2}} \right) \quad (12.240)$$

Ground effect comes into play when the wing height above the ground plane is less than about 3/4 of the wing span

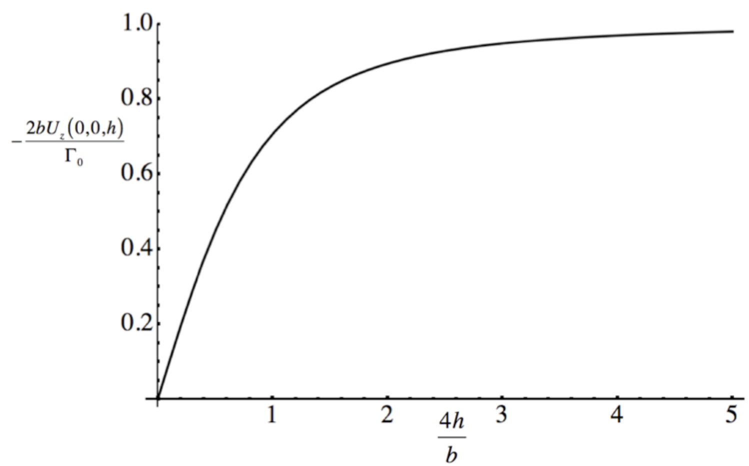

Figure 12.38 Effect of the presence of a ground plane on the downwash at the center of the lifting line.

NACA airfoil numbering system

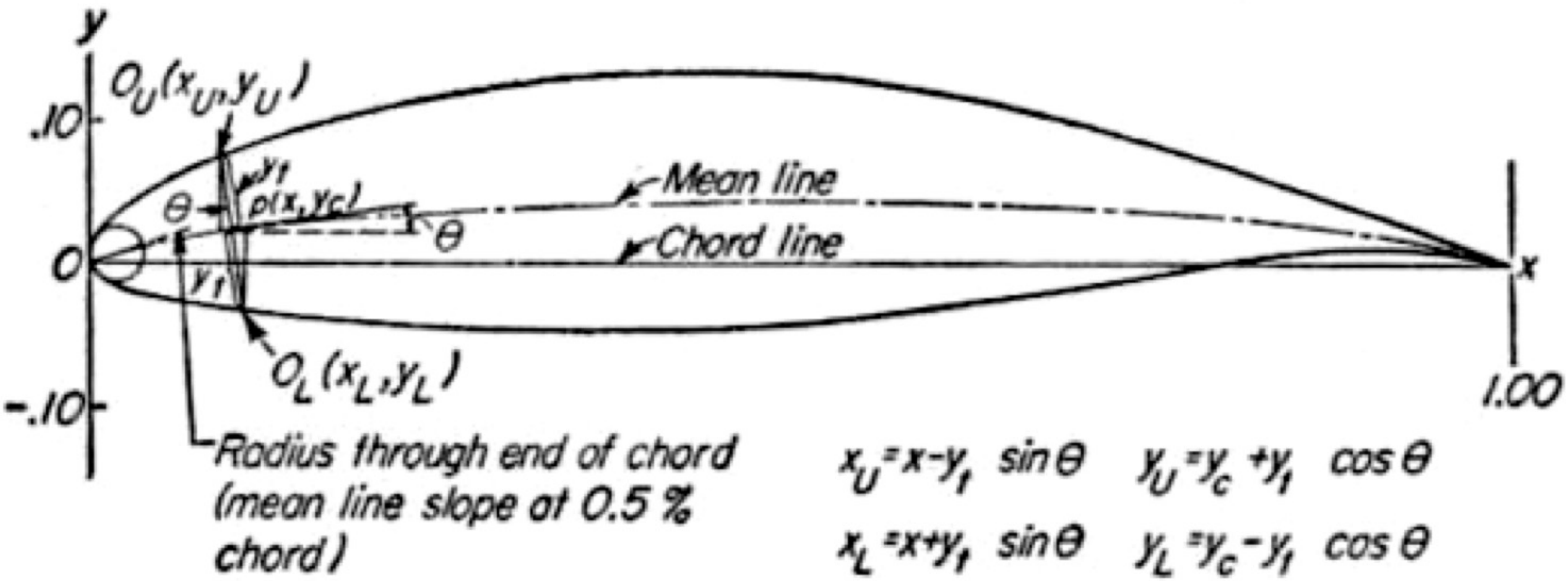

NACA airfoil geometrical construction

STANFORD
AERONAUTICS &
ASTRONAUTICS

NACA Four-Digit Series:

The first family of airfoils designed using this approach became known as the NACA Four-Digit Series. The first digit specifies the maximum camber (m) in percentage of the chord (airfoil length), the second indicates the position of the maximum camber (p) in tenths of chord, and the last two numbers provide the maximum thickness (t) of the airfoil in percentage of chord. For example, the NACA 2415 airfoil has a maximum thickness of 15% with a camber of 2% located 40% back from the airfoil leading edge (or 0.4c). Utilizing these m, p, and t values, we can compute the coordinates for an entire airfoil using the following relationships:

1. Pick values of x from 0 to the maximum chord c.
2. Compute the mean camber line coordinates by plugging the values of m and p into the following equations for each of the x coordinates.

$$y_c = \frac{m}{p^2}\left(2px - x^2\right) \qquad \text{from } x = 0 \text{ to } x = p$$

$$y_c = \frac{m}{(1-p)^2}\left[(1-2p) + 2px - x^2\right] \qquad \text{from } x = p \text{ to } x = c$$

where
x = coordinates along the length of the airfoil, from 0 to c (which stands for chord, or length)
y = coordinates above and below the line extending along the length of the airfoil, these are either y_t for thickness coordinates or y_c for camber coordinates
t = maximum airfoil thickness in tenths of chord (i.e. a 15% thick airfoil would be 0.15)
m = maximum camber in tenths of the chord
p =position of the maximum camber along the chord in tenths of chord

3. Calculate the thickness distribution above (+) and below (-) the mean line by plugging the value of t into the following equation for each of the x coordinates.

$$\pm y_t = \frac{t}{0.2}\left(0.2969\sqrt{x} - 0.1260x - 0.3516x^2 + 0.2843x^3 - 0.1015x^4\right)$$

4. Determine the final coordinates for the airfoil upper surface (x_U, y_U) and lower surface (x_L, y_L) using the following relationships.

$$x_U = x - y_t \sin\theta$$

$$y_U = y_c + y_t \cos\theta$$

$$x_L = x + y_t \sin\theta$$

$$y_L = y_c - y_t \cos\theta$$

$$\text{where } \theta = \arctan\left(\frac{dy_c}{dx}\right)$$

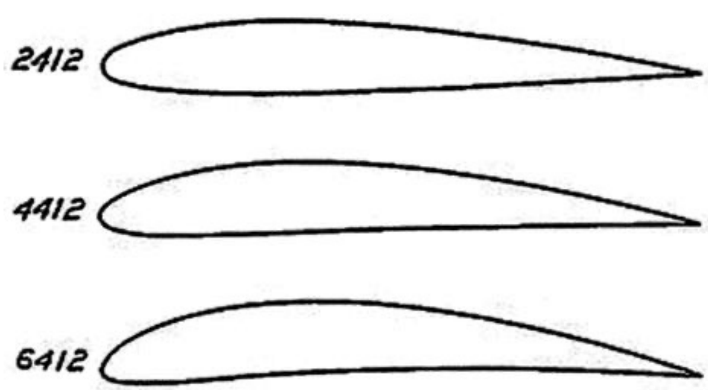

NACA Five-Digit Series:
The NACA Five-Digit Series uses the same thickness forms as the Four-Digit Series but the mean camber line is defined differently and the naming convention is a bit more complex. The first digit, when multiplied by 3/2, yields the design lift coefficient (c_l) in tenths. The next two digits, when divided by 2, give the position of the maximum camber (p) in tenths of chord. The final two digits again indicate the maximum thickness (t) in percentage of chord. For example, the NACA 23012 has a maximum thickness of 12%, a design lift coefficient of 0.3, and a maximum camber located 15% back from the leading edge. The steps needed to calculate the coordinates of such an airfoil are:

and so on …..

STANFORD
AERONAUTICS & ASTRONAUTICS

Family	Advantages	Disadvantages	Applications
4-Digit	1. Good stall characteristics 2. Small center of pressure movement across large speed range 3. Roughness has little effect	1. Low maximum lift coefficient 2. Relatively high drag 3. High pitching moment	1. General aviation 2. Horizontal tails ***Symmetrical:*** 3. Supersonic jets 4. Helicopter blades 5. Shrouds 6. Missile/rocket fins
5-Digit	1. Higher maximum lift coefficient 2. Low pitching moment 3. Roughness has little effect	1. Poor stall behavior 2. Relatively high drag	1. General aviation 2. Piston-powered bombers, transports 3. Commuters 4. Business jets
16-Series	1. Avoids low pressure peaks 2. Low drag at high speed	1. Relatively low lift	1. Aircraft propellers 2. Ship propellers
6-Series	1. High maximum lift coefficient 2. Very low drag over a small range of operating conditions 3. Optimized for high speed	1. High drag outside of the optimum range of operating conditions 2. High pitching moment 3. Poor stall behavior 4. Very susceptible to roughness	1. Piston-powered fighters 2. Business jets 3. Jet trainers 4. Supersonic jets
7-Series	1. Very low drag over a small range of operating conditions 2. Low pitching moment	1. Reduced maximum lift coefficient 2. High drag outside of the optimum range of operating conditions 3. Poor stall behavior 4. Very susceptible to roughness	Seldom used
8-Series	Unknown	Unknown	Very seldom used